Article

Cell Reports

Differential Requirement for Translation Initiation Factor Pathways during Ecdysone-Dependent Neuronal Remodeling in *Drosophila*

Graphical Abstract

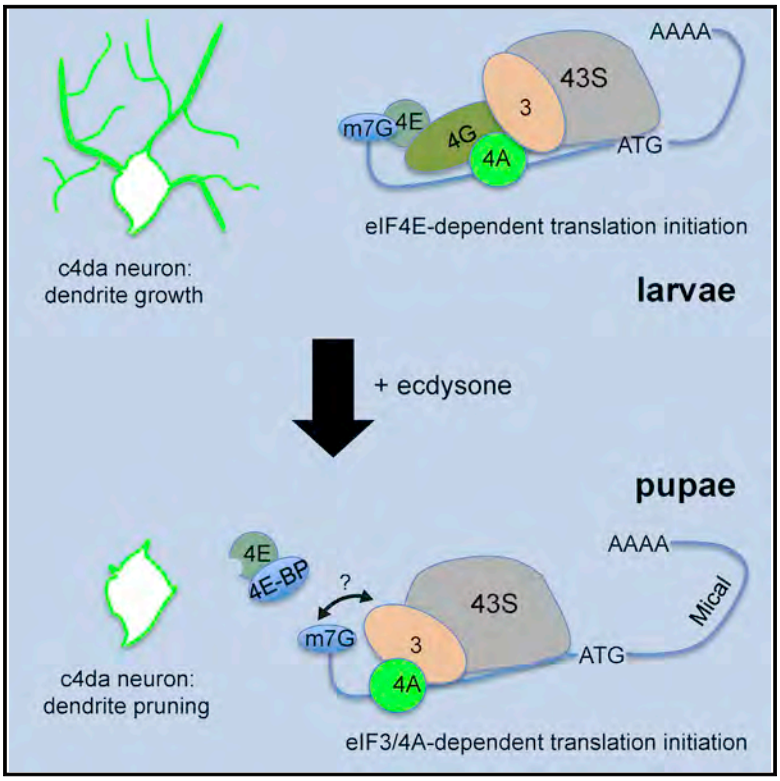

Highlights

- Dendrite pruning in the fly PNS requires eIF4A and eIF3, but not eIF4E/G
- The helicase eIF4A and eIF3 cooperate for expression of the ecdysone target Mical
- Initiation pathway choice depends on signals in the Mical 5′ UTR
- eIF3 and eIF4A seem to be linked to several ecdysone-induced processes

Authors

Sandra Rode, Henrike Ohm, Lea Anhäuser, ..., Andrea Rentmeister, Sijun Zhu, Sebastian Rumpf

Correspondence

sebastian.rumpf@uni-muenster.de

In Brief

Ecdysone regulates developmental neurite pruning in *Drosophila* through the activation of pruning genes, but it also negatively affects global translation rate. Rode et al. find that these effects are coordinated at the level of translation initiation, as pruning genes use the eIF3 initiation complex instead of the ecdysone-sensitive canonical eIF4F complex.

Rode et al., 2018, Cell Reports *24*, 2287–2299
August 28, 2018 © 2018 The Author(s).
https://doi.org/10.1016/j.celrep.2018.07.074

CellPress

Cell Reports
Article

Differential Requirement for Translation Initiation Factor Pathways during Ecdysone-Dependent Neuronal Remodeling in *Drosophila*

Sandra Rode,[1] Henrike Ohm,[1] Lea Anhäuser,[2] Marina Wagner,[3,4] Mechthild Rosing,[1] Xiaobing Deng,[5] Olga Sin,[6] Sebastian A. Leidel,[6] Erik Storkebaum,[3,4,7] Andrea Rentmeister,[2] Sijun Zhu,[5] and Sebastian Rumpf[1,8,*]

[1]Institute for Neurobiology, University of Münster, Badestrasse 9, 48149 Münster, Germany
[2]Institute for Biochemistry, University of Münster, Wilhelm-Klemm-Strasse 2, 48149 Münster, Germany
[3]Molecular Neurogenetics Laboratory, Max Planck Institute for Molecular Biomedicine, Von-Esmarch-Strasse 54, 48149 Münster, Germany
[4]Faculty of Medicine, University of Münster, 48149 Münster, Germany
[5]Department of Neuroscience and Physiology, State University of New York Upstate Medical University, Syracuse, NY 13210, USA
[6]Max Planck Research Group for RNA Biology, Max Planck Institute for Molecular Biomedicine, Von-Esmarch-Strasse 54, 48149 Münster, Germany
[7]Present address: Department of Molecular Neurobiology, Donders Institute for Brain, Cognition and Behaviour, Radboud University, Nijmegen, the Netherlands
[8]Lead Contact
*Correspondence: sebastian.rumpf@uni-muenster.de
https://doi.org/10.1016/j.celrep.2018.07.074

SUMMARY

Dendrite pruning of *Drosophila* sensory neurons during metamorphosis is induced by the steroid hormone ecdysone through a transcriptional program. In addition, ecdysone activates the eukaryotic initiation factor 4E-binding protein (4E-BP) to inhibit cap-dependent translation initiation. To uncover how efficient translation of ecdysone targets is achieved under these conditions, we assessed the requirements for translation initiation factors during dendrite pruning. We found that the canonical cap-binding complex eIF4F is dispensable for dendrite pruning, but the eIF3 complex and the helicase eIF4A are required, indicating that differential translation initiation mechanisms are operating during dendrite pruning. eIF4A and eIF3 are stringently required for translation of the ecdysone target Mical, and this depends on the 5′ UTR of Mical mRNA. Functional analyses indicate that eIF4A regulates eIF3-mRNA interactions in a helicase-dependent manner. We propose that an eIF3-eIF4A-dependent alternative initiation pathway bypasses 4E-BP to ensure adequate translation of ecdysone-induced genes.

INTRODUCTION

Pruning, the developmentally controlled degeneration of synapses and neurites without loss of the parent neuron, is an important mechanism used to specify neuronal connections or to remove developmental intermediates (Luo and O'Leary, 2005; Schuldiner and Yaron, 2015). In holometabolous insects like *Drosophila*, the nervous system is remodeled during metamorphosis in response to the steroid hormone ecdysone. In the peripheral nervous system (PNS), the sensory class IV dendritic arborization (c4da) neurons completely prune their long and branched larval dendrites at the onset of the pupal phase, while their axons stay intact (Kuo et al., 2005; Williams and Truman, 2005). C4da neuron dendrite pruning involves the specific destabilization of the dendritic cytoskeleton and plasma membrane (Herzmann et al., 2017, 2018) and phagocytosis of severed dendrites by surrounding epidermal cells (Han et al., 2014).

Ecdysone induces c4da neuron dendrite pruning through the hormone receptors EcR-B1 and ultraspiracle (Usp), which activate the transcription of pruning genes (Kuo et al., 2005; Williams and Truman, 2005). Among these are *headcase*, a pruning gene of unknown function (Loncle and Williams, 2012), and *SOX14*, an HMG box transcription factor that activates transcription of *MICAL*, encoding an actin-severing enzyme (Kirilly et al., 2009). Regulation of *MICAL* expression also involves the ubiquitin-proteasome system at a posttranscriptional level (Rumpf et al., 2014).

In addition to transcriptional activation of target genes, several lines of evidence suggest that ecdysone also regulates global translation rates through activation of the translation inhibitor eukaryotic initiation factor 4E-binding protein (4E-BP). In the *Drosophila* fat body, this occurs transcriptionally through FOXO (Colombani et al., 2005), while in c4 da neurons, ecdysone inhibits the insulin and Target of Rapamycin (TOR) pathway to activate 4E-BP posttranslationally (Wong et al., 2013).

4E-BP inhibits translation initiation, the rate-limiting step of protein synthesis, by sequestering the cap-binding protein eIF4E (Gingras et al., 1999). During canonical translation initiation, eIF4E binds to the 7-methylguanosine (m^7Gppp) cap of eukaryotic mRNAs and then forms the so-called eIF4F complex by recruiting eIF4G, an adaptor that binds the 43S preinitiation complex (PIC), containing the 40S small ribosomal subunit, and the helicase eIF4A, which is thought to resolve hairpin structures in the 5′ UTRs of mRNAs (Svitkin et al., 2001; Wolfe et al., 2014). This enables the 43S complex to scan 5′ UTRs for the initiation

codon, where it is joined by the large ribosomal subunit and translation can start (Hinnebusch, 2014). While eIF4A's role has been mainly linked to 5′ UTR hairpins, it can also stimulate translation of mRNAs with unstructured 5′ UTRs (Yourik et al., 2017). Moreover, eIF4A is more abundant than eIF4E (Gingras et al., 1999), suggesting that it has functions beyond the eIF4F complex.

Activated 4E-BP binds to eIF4E and prevents eIF4F assembly, thus inhibiting ribosome recruitment to mRNAs and globally dampening translation rates under stress or during development (Gingras et al., 1999; Richter and Sonenberg, 2005). Interestingly, 4E-BP affects translation of some mRNAs more than others (Gandin et al., 2016; Hsieh et al., 2012). To explain this, eIF4E-independent translation initiation mechanisms have been proposed. One such mechanism could depend on internal ribosome entry sites (IRESs) that bypass the requirement for the m^7Gppp cap (Yamamoto et al., 2017). For example, the mRNAs of the *Drosophila* cell death factors *reaper* and *hid* may contain IRES sequences in their 5′ UTRs that allow them to be translated under stress (Hernández et al., 2004; Vazquez-Pianzola et al., 2007).

Alternative cap recognition mechanisms have also been proposed under conditions of high 4E-BP activity. In particular, the initiation factor eIF3, a 13-subunit complex, could provide a mechanism for eIF4E-independent initiation (Lee et al., 2015, 2016). It binds to the small ribosomal subunit as part of the 43S PIC, and it is thought to act downstream of eIF4G in mRNA recruitment. However, eIF3 dependence varies between mRNAs, and eIF3 can even suppress translation of some targets (Lee et al., 2015). Importantly, it was recently shown that translation of some 4E-BP-resistant mRNAs depends on an eIF3-based cap recognition activity in the eIF3d subunit that is stimulated by hairpin motifs in the 5′ UTR (Lee et al., 2016). Other eIF3 subunits have also been shown to interact with the cap (Kumar et al., 2016).

Given that ecdysone inhibits eIF4E-dependent translation, we asked whether there are mechanisms that ensure the translation of ecdysone target mRNAs. To this end, we assessed the requirements for translation initiation factors during c4da neuron dendrite pruning. We found that the canonical eIF4F components eIF4E and eIF4G are not required for c4da neuron dendrite pruning, while the helicase eIF4A and the eIF3 complex are. Both eIF4A and eIF3 are required for Mical expression, and this specificity is conferred by the 5′ UTR of Mical mRNA. Further biochemical analyses suggest that eIF4A regulates the interaction between eIF3 and the Mical 5′ UTR. We propose that eIF4A/eIF3 constitute a 4E-BP bypass mechanism that ensures the adequate translation of ecdysone-induced genes in c4da neurons.

RESULTS

eIF4A, but Not eIF4E, Is Required for Sensory Neuron Dendrite Pruning

To address the requirements for translation initiation factors during dendrite pruning, we expressed transgenic double-stranded RNA (dsRNA) constructs against the three eIF4F subunits in c4da neurons under the control of *ppk-GAL4*. C4da neurons have long and branched dendrites at the larval stage (Figure 1A), which are pruned completely at 18 hr after puparium formation (APF) (Figure 1B). Transgenic RNAi constructs against eIF4E1, eIF4G1, and the eIF4A-activating protein eIF4B did not cause defects in c4da neuron dendrite pruning (Figures S1A–S1G and S1K). Ubiquitous knockdown of eIF4E1 and eIF4G1 under the driver *actin-GAL4* caused lethality (Table S1), indicating that the dsRNAs were functional. In contrast, expression of three dsRNA constructs directed against *Drosophila* eIF4A caused strong pruning defects, with up to 95% of c4da neurons retaining dendrites attached to the cell body at 18 hr APF (Figures S1H–S1J and S1K).

To confirm these results, we next inhibited eIF4F by overexpressing constitutively active 4E-BP (*UAS-4E-BP^{LL}*) (Miron et al., 2001). Consistent with previous results (Niehues et al., 2015), 4E-BP^{LL} caused a reduction of larval dendrites compared to controls (Figures 1A, 1B, and 1F). However, dendrites of 4E-BP^{LL}-expressing c4da neurons were pruned largely normally at 18 hr APF (Figures 1A', 1B', 1G, and 1H). C4da neurons homozygous for the previously characterized strong P-element mutation *eIF4E1^{s058911}* (Lachance et al., 2002) generated by MARCM (Lee and Luo, 1999) also did not show pruning defects (Figures 1C', 1G, and 1H).

To confirm that loss of eIF4A causes pruning defects, we generated a UAS line expressing an eIF4A variant with a mutation in the DEAD box motif (*eIF4A^{E172Q}*). Expression of this ATPase-dead eIF4A in c4 da neurons caused strong dominant dendrite-pruning defects (Figures 1D', 1G, and 1H). Further, homozygous *eIF4A^{1006}* mutant c4 da neurons generated by MARCM also showed strong dendrite-pruning defects (Figures 1E, 1E', 1G, and 1H).

As the strong eIF4A manipulations caused a decrease in the number of larval dendrites (Figure 1F), we sought to exclude that the pruning defects were caused by pre-existing defects. To this end, we used a drug-inducible ppk-*GeneSwitch* driver (Osterwalder et al., 2001) to activate *UAS-eIF4A^{E172Q}* expression in c4 da neurons only 24 hr before the pupal stage, at a time when larval dendrites are well elaborated. Short-term induction of *eIF4A^{E172Q}* caused dendrite-pruning defects indistinguishable from those caused by constitutive expression (Figures S1L and S1M). These results suggest that eIF4E-independent translation initiation mechanisms are important for c4 da neuron dendrite pruning and that eIF4A is required for dendrite pruning independently of the eIF4F complex.

eIF4A Requirement during Pruning Cannot Be Explained by an Effect on Global Translation Rate

To assess translation rates in c4da neurons, we used fluorescent noncanonical amino acid tagging (FUNCAT) (Erdmann et al., 2015). Briefly, we expressed a variant methionyl-tRNA synthetase in c4da neurons to allow incorporation of the noncanonical amino acid azidonorleucine (ANL) into newly translated proteins. Proteins labeled in this way can be fluorescently tagged via click chemistry (Erdmann et al., 2015). Third instar larvae expressing variant methionyl-tRNA synthetase in c4da neurons were placed on ANL-containing medium for 48 hr, dissected, and click-labeled with TAMRA dye. Incorporated TAMRA was then visualized by confocal microscopy in animals

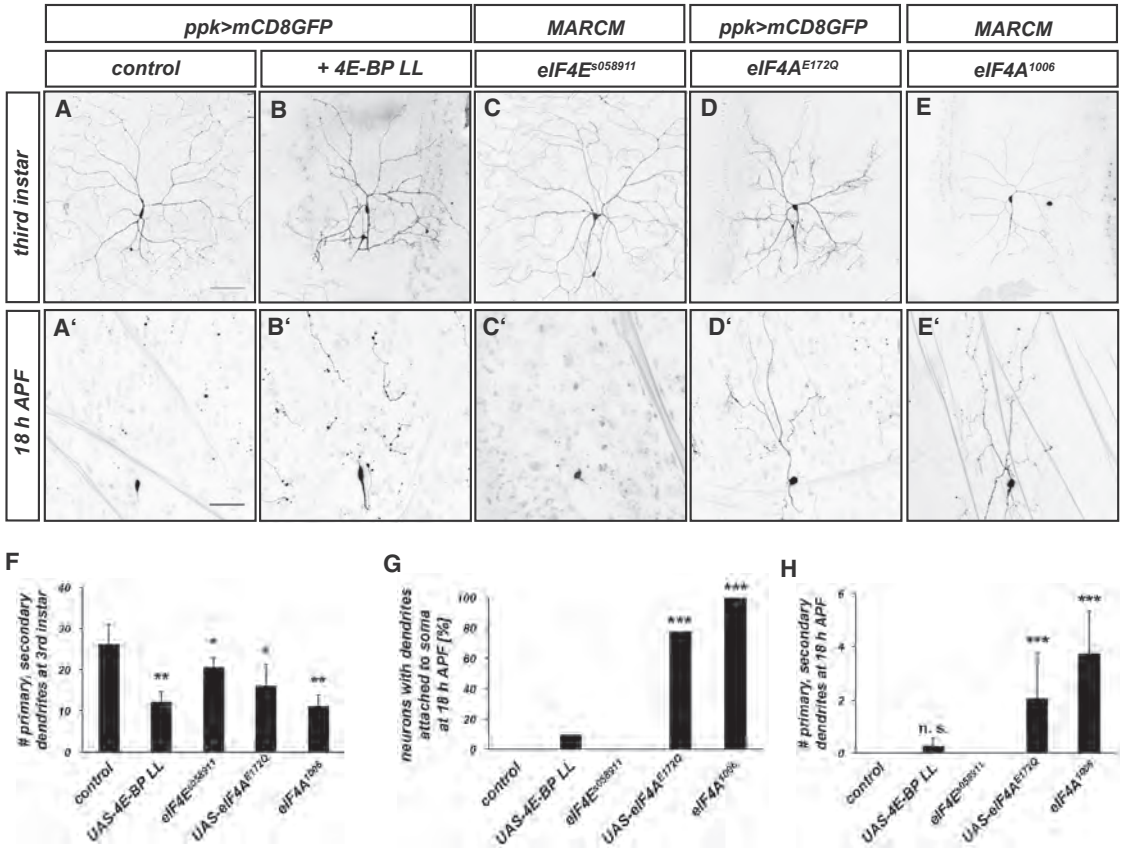

Figure 1. eIF4A Is Required for c4da Neuron Dendrite Pruning Independently of the Canonical eIF4F Complex

(A–E) c4da neurons of the indicated genotypes at the third instar larval stage; (A')–(E') show c4da neurons at 18 hr APF. (A and A') Control c4da neurons labeled by CD8::GFP expressed under *ppk-GAL4*. (B and B') c4da neurons expressing constitutively active *4E-BP LL*. (C and C') *eIF4E*^{s058911} c4da MARCM clones labeled by expression of mCD8::GFP. (D and D') c4da neurons expressing ATPase-dead *eIF4A*^{E172Q} under *ppk-GAL4*. (E and E') *eIF4A*^{1006} c4 da MARCM clones labeled by the expression of tdtomato.

(F) Number of primary and secondary dendrites attached to the cell body at third instar in (A)–(E) (n = 15–42). *p < 0.05, ***p < 0.001, Wilcoxon test.

(G) Penetrance of pruning defects in (A')–(E'). ***p < 0.001, Fisher's exact test.

(H) Number of primary and secondary dendrites attached to the cell body at 18 hr APF. ***p < 0.001, Wilcoxon test. Data in (F) and (H) are mean ± SD. Scale bars, 100 μm (A–E) and 50 μm (A'–E').

See also Figures S1 and S2.

expressing control or eIF4A dsRNA constructs and quantified (Figures S2A and S2B). Knockdown of eIF4A reduced the amount of newly translated proteins by approximately 40% (Figure S2E). We then expressed constitutively active 4E-BP^{LL} in c4 da neurons to inhibit eIF4E. This had previously been shown to strongly decrease translation rates (Niehues et al., 2015). 4E-BP^{LL} reduced translation rates to a similar degree as eIF4A knockdown (Figures S2C, S2D, and S2F). As the inhibition of eIF4A and eIF4E has very different effects on c4da neuron dendrite pruning, our data suggest that these two factors regulate different sets of mRNAs.

The eIF3 Complex Is Required for Dendrite Pruning

The lack of pruning defects upon inhibition of core eIF4F components was surprising because dendrite pruning requires expression of several pruning factors. We therefore hypothesized that alternative translation initiation factors may be required instead. A candidate component of such a pathway is the initiation factor eIF3, a large 13-subunit complex that is thought to cooperate with eIF4G in ribosome recruitment during canonical translation initiation (Cate, 2017). eIF3 was recently shown to participate in eIF4E-independent modes of translation initiation (Lee et al., 2016; Meyer et al., 2015) (see also Figure 7 for model).

To test whether eIF3 is important for c4da neuron dendrite pruning, we expressed dsRNA constructs directed against its core subunits eIF3c and eIF3e in c4 da neurons. Knockdown of these two factors caused strong c4da neuron dendrite-pruning defects at 18 hr APF (Figures 2A–2C', 2F, and 2G). Furthermore, homozygous *eIF3g1*^{A} or *eIF3b*^{EY14430} mutant c4da neuron clones generated by MARCM also displayed strong dendrite pruning defects at 18 hr APF (Figures 2D–2G).

eIF3 may also contribute to eIF4E-independent translation initiation through a recently discovered cap-binding activity in its eIF3d subunit (Lee et al., 2016). To address whether this

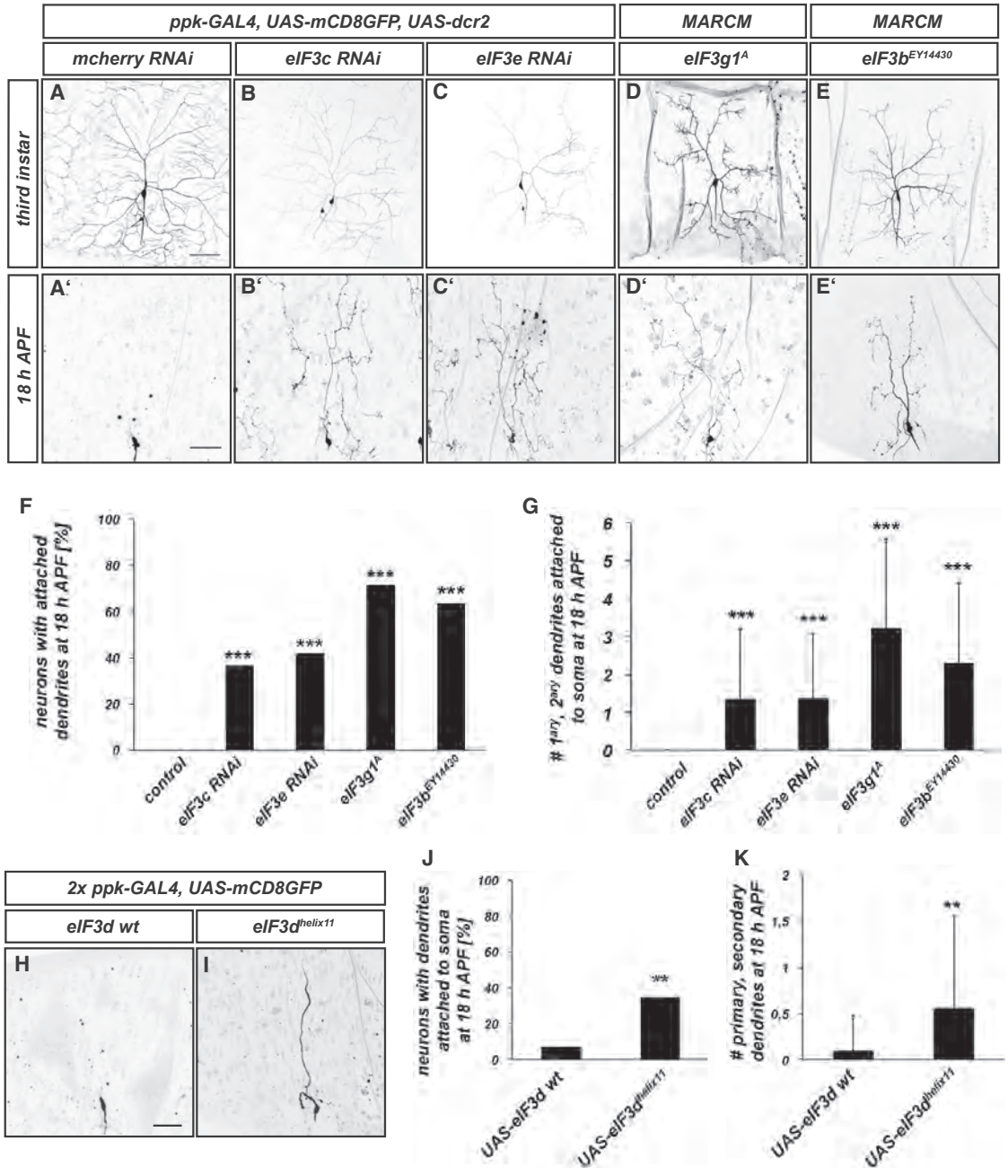

Figure 2. The eIF3 Complex Is Required for Translation Initiation during c4da Neuron Dendrite Pruning

(A–E) c4da neurons of the indicated genotypes at the third instar larval stage; (A')–(E') show c4da neurons at 18 hr APF. (A and A') Control c4da neurons labeled by CD8::GFP expressed under *ppk-GAL4*. (B and B') c4da neurons expressing eIF3c RNAi. (C and C') c4da neurons expressing eIF3e RNAi. (D and D') *eIF3g1*^{A} c4da MARCM clones labeled by the expression of CD8GFP. (E and E') *eIF3b*^{EY14430} c4da MARCM clones labeled by the expression of tdtomato.

(F) Penetrance of pruning defects in (A')–(D'). ***$p < 0.001$, Fisher's exact test (n = 11–30).

(G) Number of primary and secondary dendrites attached to the cell body at 18 hr APF. Data are mean ± SD. ***$p < 0.001$, Wilcoxon test.

(H–K) Dominant effects of an eIF3d cap-binding mutant on c4da neuron dendrite pruning. Wild-type eIF3d (H) or the cap-binding mutant eIF3d^{helix11} (I) were overexpressed in c4da neurons, and pruning defects were assessed at 18 hr APF. (J) Penetrance of dendrite-pruning defects in (H) and (I) (n = 42–75). **$p < 0.01$, Fisher's exact test. (K) Number of primary and secondary dendrites attached to the cell body at 18 hr APF in (H) and (I). Data are mean ± SD. **$p < 0.01$, Wilcoxon test. Scale bars, 100 μm (A–E) and 50 μm (A'–E' and H).

activity contributes to eIF3 function during dendrite pruning, we generated a *UAS-eIF3d* construct containing mutations in the cap-binding domain. This mutant, termed eIF3d^{helix11}, had previously been shown to prevent recruitment of a specific target mRNA to the 43S PIC *in vitro* (Lee et al., 2016). While overexpression of wild-type eIF3d in c4da neurons did not cause dendrite-pruning defects (Figure 2H), overexpression of eIF3d^{helix11} caused more than 30% of c4da neurons to retain dendrites at 18 hr APF (Figure 2I). This effect was weaker than those of eIF3 knockdowns or mutants (Figures 2J and 2K), likely because such dominant-negative approaches can be ineffective or because additional functions of eIF3 also contribute to pruning. Nevertheless, our phenotypic data suggest that eIF3 is required for translation initiation of crucial dendrite pruning factors in c4da neurons during the early pupal phase. Moreover, the fact that an eIF3 cap-binding mutant caused dominant pruning defects suggests that c4da neuron dendrite pruning relies on cap-dependent translation initiation.

eIF4A and eIF3 Are Required for Mical Expression

The above data suggest that eIF4A and eIF3, but not eIF4E/G, are required for translation initation of dendrite pruning factors during the early pupal phase. To identify such targets, we next assessed the expression of known ecdysone-induced pruning factors during the early pupal stage by immunofluorescence. The ecdysone receptor EcR-B1 is activated at the onset of the pupal stage and activates transcription of target genes, such as *SOX14* and *headcase* (Kirilly et al., 2009; Loncle and Williams, 2012). Sox14 in turn activates transcription of Mical (Kirilly et al., 2009).

Expression of EcR-B1 and headcase in c4da neurons was not affected by eIF4A downregulation (Figures S3A–S3D). We therefore focused on the Sox14-Mical branch of the transcriptional cascade. At 2 hr APF, Sox14 expression in c4da neurons was affected neither by the expression of 4E-BP^{LL} to inhibit eIF4E (Figures 3A and 3B) nor by eIF4A manipulation (*eIF4A* RNAi, the *eIF4A*^{1006} mutation, or expression of *eIF4A*^{E172Q}) (Figures 3C–3E). Furthermore, Sox14 was also present in c4da neurons expressing dsRNA constructs against eIF3c or eIF3e (Figures 3F and 3G).

We next assessed the effects of translation initation factor manipulations on Mical protein expression at 2 hr APF. Mical expression was not affected by eIF4E inhibition (Figures 3A' and 3B'), but it was strongly reduced by all tested eIF4A manipulations (*eIF4A* RNAi, the *eIF4A*^{1006} mutation, or expression of *eIF4A*^{E172Q}) (Figures 3C'–3E') and upon knockdown of eIF3c and eIF3e (Figures 3F' and 3G'). Thus, eIF4A and eIF3 might be required for c4 da neuron dendrite pruning through a specific role in pruning gene expression.

To explain why Sox14 was unaffected by manipulations of both the eIF4F complex and eIF3, we reasoned that redundant translation initiation pathways might exist for Sox14 mRNA. Indeed, simultaneous inhibition of eIF4E (by 4E-BP^{LL}) and eIF3 (by eIF3e knockdown) abrogated Sox14 expression (Figure 3H). Taken together, eIF4A and eIF3 appear to have similar target preferences during c4da neuron dendrite pruning, as they are both specifically required for Mical expression. Sox14 translation, on the other hand, can be initiated by either an eIF4E- or an eIF3-dependent mechanism.

Mical Is a Major Target for eIF4A and eIF3 during c4 da Neuron Dendrite Pruning

Given that eIF4A and eIF3 were stringently required for Mical expression, we wondered whether loss of Mical expression was a major cause for the pruning defects upon loss of eIF4A or eIF3. We therefore tested whether we could rescue these pruning defects by upregulation of Mical. To this end, we attempted to rescue the pruning defects caused by eIF3-eIF4A manipulations by overexpression of a transgenic Mical construct harboring all crucial domains (Terman et al., 2002) (herafter called Mical^{FL} for full length) or Mical$^{\Delta C}$, a truncated version of Mical insufficient for pruning (Kirilly et al., 2009). Coexpression of eIF4A dsRNA with tdtomato caused approximately 70% of c4da neurons to retain dendrites attached to the soma at 18 hr APF (Figures 4A, 4D, and 4E). Remarkably, overexpression of Mical^{FL}, but not Mical$^{\Delta C}$, strongly reduced both the penetrance and severity of these pruning defects (Figures 4B–4E). A similar suppression was also seen upon coexpression of a GFP-tagged Mical^{FL} transgene (Hung et al., 2010), but not upon coexpression of Mical mutants lacking the calponin homology region or the flavoprotein monooxygenase domain encoding the active site for actin oxidation (Figure S4).

We next assessed the relationship between eIF3 and Mical by the same strategy. Silencing eIF3e expression led to the retention of dendrites attached to the soma in approximately 70% of c4da neurons at 18 hr APF (Figure 4F). Remarkably, Mical^{FL} overexpression was again able to rescue the pruning defects induced by eIF3e knockdown, while Mical$^{\Delta C}$ was not (Figures 4G–4J). Thus, Mical is an important target of both eIF4A and eIF3 during c4da neuron dendrite pruning.

Exogenous Sox14 activates transcription of the endogenous Mical gene and can bypass the pruning defects of several mutants with defects in ecdysone-dependent gene expression (Kirilly et al., 2009; Rumpf et al., 2014). Interestingly, Sox14 overexpression in neurons expressing eIF4A dsRNA caused a decrease in the length of unpruned dendrites at 18 hr APF, but it did not lead to a decrease in the penetrance of the defects, indicating that mere transcriptional upregulation of endogenous Mical could not reduce the severing defects caused by the loss of eIF4A (Figure S4) (see also below).

eIF4A/eIF3 Dependence Is Conferred by the 5′ UTR of Mical mRNA

What are the signals that render Mical expression dependent on eIF4A and eIF3? Both eIF4A and eIF3 interact with the 5′ UTRs of their target mRNAs during translation initiation (Hinnebusch, 2014). The cap-binding activity of eIF3d also requires specific secondary structures in the 5′ UTRs of a target mRNA (Lee et al., 2016). An involvement of the Mical 5′ UTR would also be consistent with the above data showing that induction of endogenous Mical mRNA via Sox14 (i.e., containing the endogenous 5′ UTR) cannot rescue the eIF4A knockdown phenotype (Figure S4).

To address whether the Mical 5′ UTR (256 bp) is a determinant of eIF4A/eIF3 dependence, we characterized it in different reporter assays. We first used *in vitro* transcription to generate a *5′ UTR^{Mical}-Luciferase* reporter mRNA for *in vitro* translation experiments. Translation of this reporter mRNA in reticulocyte lysate yielded robust luciferase activity when the mRNA was

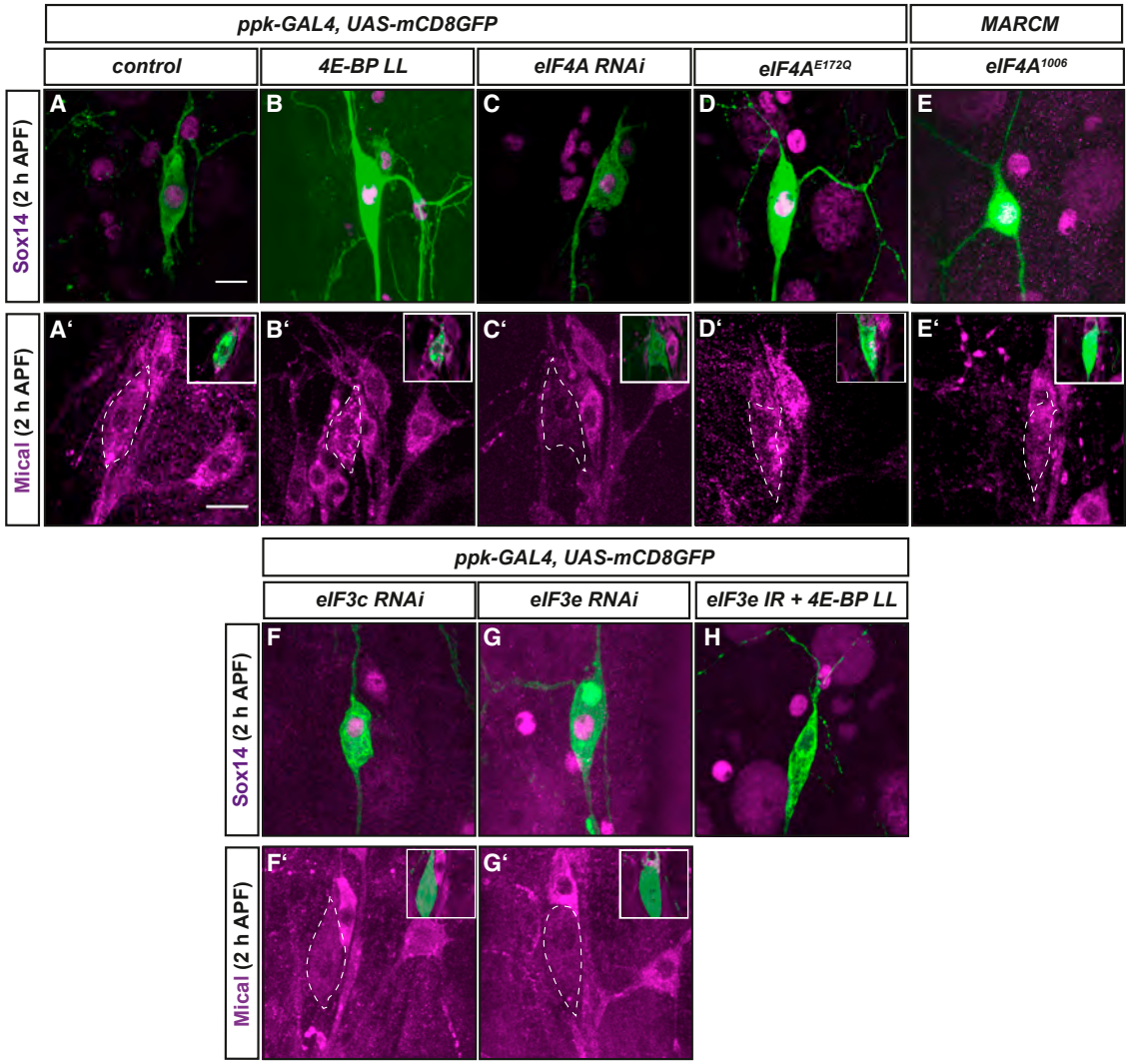

Figure 3. Effects of Initiation Factor Manipulations on Ecdysone Target Gene Expression

(A–H) Pupal filets at 2 hr APF were stained with antibodies against Sox14 (A–H) or Mical (A'–G') (magenta), and c4 da neurons were labeled with CD8GFP under *ppk-GAL4* or tdtomato in MARCM clones. (A–H) The merge of Sox14 stainings (magenta) and neuron marker (green) is shown. (A'–G') Only the Mical stainings are shown in the large panels, and the merge with the neuron markers is shown in insets. (A and A') Control c4da neuron. (B and B') c4da neuron expressing 4E-BP LL. (C and C') c4da neuron expressing eIF4A RNAi. (D and D') c4da neuron expressing *eIF4A*^{E172Q}. (E and E') Homozygous *eIF4A*^{1006} c4da MARCM clone. (F and F') c4da neuron expressing eIF3c RNAi. (G and G') c4da neuron expressing eIF3e RNAi. (H) c4da neuron expressing 4E-BP LL and eIF3e RNAi. Scale bars, 10 μm. See also Figure S3.

capped with the functional cap analog ARCA ($m_2^{7,3'}$-OGpppG), but not when the mRNA was capped with the inactive cap analog ApppG (Figure S5A). Thus, *5′ UTR*^{Mical} requires a functional cap in order to promote translation initiation.

We next generated a UAS-*5′ UTR*^{Mical}-GFP reporter for *in vivo* studies. In control third instar c4da neurons, *UAS-5′ UTR*^{Mical}*-GFP* yielded robust fluorescence (Figure 5A). In keeping with our above results, expression from *5′ UTR*^{Mical}*-GFP* was not affected by 4E-BP^{LL} overexpression to inhibit eIF4E (Figures 5B and 5E). Likewise, expression of a *UAS-GFP* reporter was not affected by 4E-BP^{LL} (Figures 5C–5G).

We next assessed the effects of downregulation of eIF4A and eIF3. Expression from *5′ UTR*^{Mical}*-GFP* was significantly reduced upon eIF4A knockdown (Figures 5H, 5I, and 5L) and even more so in *eIF4A*^{1006} mutant c4da neuron MARCM clones (Figures S5B and S5C). *UAS-GFP* expression was also reduced by eIF4A knockdown (Figures 5J, 5K, and 5M), but to a lower degree than *UAS-5′ UTR*^{Mical}*-GFP* (Figure 5N).

Knockdown of eIF3e attenuated *5′ UTR*^{Mical}*-GFP* activity even more strongly than eIF4A knockdown (Figures 5O, 5P, and 5S). *UAS-GFP* expression was also reduced by eIF3e knockdown, but again less severely than *UAS-5′ UTR*^{Mical}*-GFP* (Figures 5Q, 5R, 5T, and 5U).

Surprisingly, the fluorescence intensity of the *UAS-tdtomato* reporter used to label c4 da neurons in these experiments was consistently upregulated upon knockdown of eIF4A and eIF3e

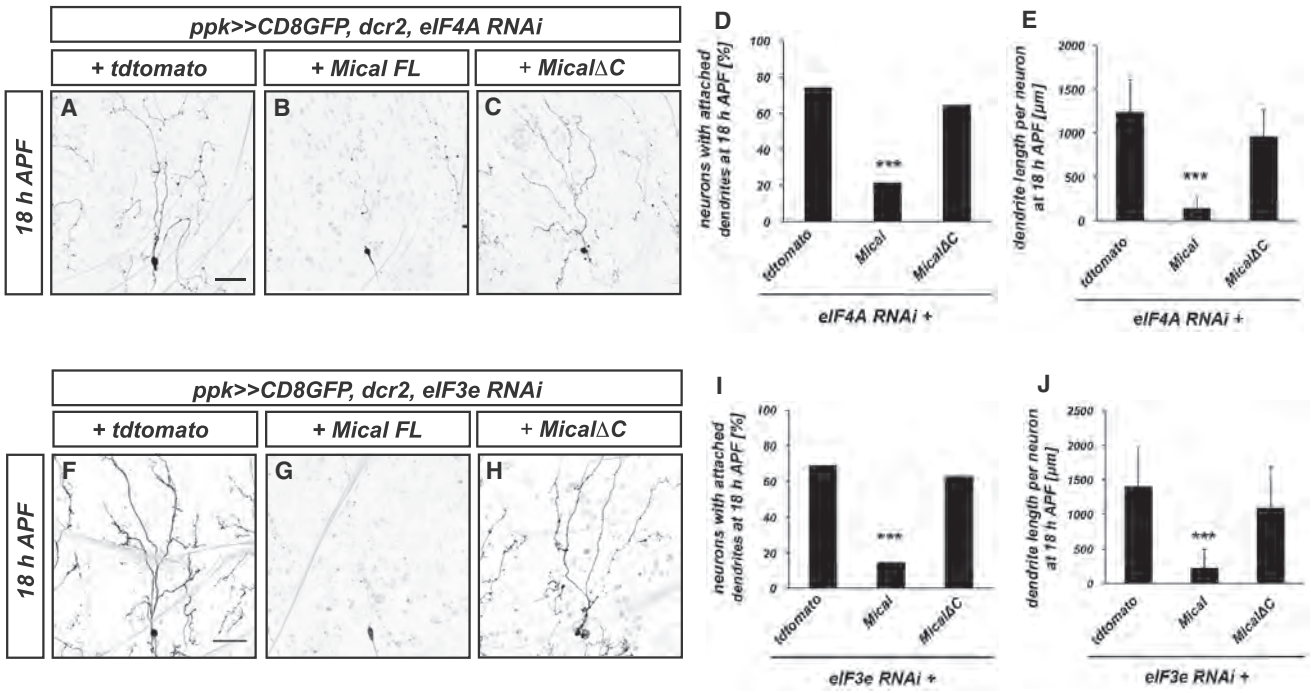

Figure 4. Mical Overexpression Rescues the Pruning Defects Induced by eIF4A or eIF3 Knockdown

RNAi constructs against eIF4A or eIF3e were expressed in c4 da neurons under the control of *ppk-GAL4*, and the effects of coexpression of the indicated UAS transgenes on dendrite pruning was assessed at 18 hr APF.

(A–C) eIF4A RNAi was coexpressed with UAS-tdtomato as dosage control (A), with full-length Mical (B), or with inactive truncated MicalΔC (C).

(D) Penetrance of dendrite-pruning defects in (A)–(C).

(E) Severity of dendrite-pruning defects in (A)–(C) as assessed by the number of attached primary and secondary dendrites.

(F–H) Genetic interactions between eIF3 and Mical. eIF3e RNAi was coexpressed with UAS-tdtomato as dosage control (F), with full-length Mical (G), or with inactive truncated MicalΔC (H).

(I) Penetrance of dendrite-pruning defects in (F)–(H).

(J) Severity of dendrite-pruning defects in (F)–(H) as assessed by the number of attached primary and secondary dendrites. In (D) and (I), ***$p < 0.001$, Fisher's exact test. In (E) and (J), data are represented as mean ± SD. ***$p < 0.001$, Wilcoxon test; n = 12–32. Scale bars, 50 μm.

See also Figure S4.

(Figure S6). This reporter gene carries additional sequences in its 5′ UTR designed to strengthen expression (Han et al., 2014) that might confer a different sensitivity to initiation factors. Indeed, eIF3 has been shown to act inhibitory on some mRNAs (Lee et al., 2015).

Taken together, our data suggest that the 5′ UTRs of the tested reporter genes confer differential dependence on eIF4A and eIF3. Since expression from the *5′ UTR^{Mical}* reporter was more strongly reduced by eIF4A/eIF3e knockdown than that of the regular UAS-GFP reporter, we conclude that the 5′ UTR of Mical mRNA encodes a signal for an eIF4A/eIF3-dependent initiation pathway.

eIF4A Regulates eIF3 Interactions with the Mical 5′ UTR

The phenotypic similarities caused by manipulations of eIF4A and eIF3 suggested that these two initiation factors cooperate closely during translation initiation of Mical mRNA. To explore this possibility further, we performed biochemical experiments in S2 cells. We first asked whether eIF4A and eIF3 are found in a complex. To this end, we transfected S2 cells with FLAG-tagged eIF4A or ATPase-dead eIF4A^{E172Q}, and we performed immunoprecipitations using anti-FLAG antibodies. We then probed the precipitates for the presence of eIF3 using an antibody against eIF3b. eIF3b could be readily detected in precipitates from cells expressing wild-type ^{FLAG}*eIF4A*, but its amount was strongly reduced when cells expressed ^{FLAG}*eIF4A^{E172Q}* (Figure 6A), suggesting an ATPase-dependent interaction between the two factors. This potential ATPase dependence of the eIF3-eIF4A interaction is in keeping with the previous notion that PIC recruitment of natural mRNAs with folded 5′ UTRs requires the eIF4A ATPase (Yourik et al., 2017; Sokabe and Fraser, 2017).

eIF3 is thought to interact with the 5′ ends of mRNAs in several ways. As part of the 43S PIC, it can bind to 5′ UTRs directly via several subunits (Lee et al., 2015). In addition, eIF3 can bind to the m^{7}Gppp cap via the subunit eIF3d (Lee et al., 2016) and possibly eIF3l (Kumar et al., 2016). However, these cap interactions are likely to be specifically regulated by *cis*-acting 5′ UTR sequences (Lee et al., 2016). In support of this notion, we did not detect eIF3 subunits or eIF4A in pull-down with m^{7}GTP-agarose, both from control and ecdysone-treated samples (Figure S7). We therefore next assessed in more detail the interactions among eIF3, eIF4A, and their natural target, the

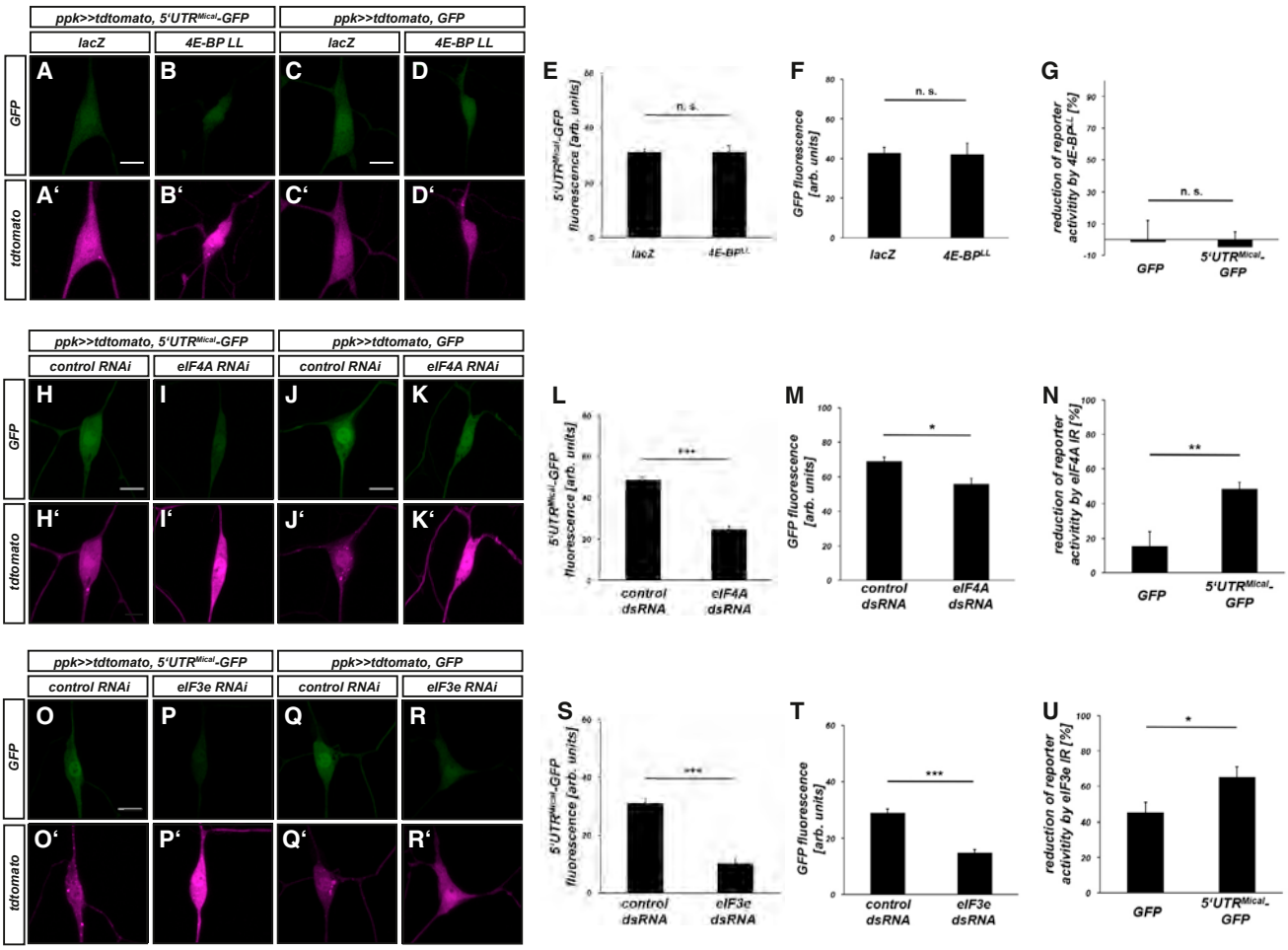

Figure 5. The Mical 5′ UTR Confers eIF4A/eIF3 Dependence

The effects of eIF4A and eIF3 manipulation on a GFP reporter gene containing the Mical 5′ UTR (*UAS-5′ UTR^{Mical}-GFP*) was assessed in third instar c4 da neurons. A regular *UAS-GFP* reporter served as a control. (A)–(D), (H)–(K), and (O)–(R) show GFP reporter signals, and (A')–(D'), (H')–(K'), and (O')–(R') show tdtomato signal in the same neurons.

(A and B) GFP intensity of *UAS-5′ UTR^{Mical}-GFP* in c4da neurons expressing UAS-lacZ as control (A) or c4da neurons expressing 4E-BP^{LL} (B).

(C and D) Intensity of *UAS-GFP* in c4da neurons expressing UAS-lacZ (C) or expressing 4E-BP^{LL} (D).

(E) GFP intensities of *5′ UTR^{Mical}-GFP* reporters in (A) and (B).

(F) GFP intensities of regular *GFP* reporters in (C) and (D).

(G) The reduction of GFP intensities of *UAS-5′ UTR^{Mical}-GFP* and *UAS-GFP* by 4E-BP^{LL} was calculated relative to controls.

(H and I) GFP intensity of *UAS-5′ UTR^{Mical}-GFP* in c4da neurons expressing a control RNAi (H) or eIF4A RNAi (I).

(J and K) GFP intensity of *UAS-GFP* in c4da neurons expressing a control RNAi (J) or eIF4A RNAi (K).

(L) GFP intensities of *5′ UTR^{Mical}-GFP* reporters in (H) and (I).

(M) GFP intensities of regular *GFP* reporters in (J) and (K).

(N) Reduction of GFP intensities of *UAS-5′ UTR^{Mical}-GFP* and *UAS-GFP* by eIF4A knockdown.

(O and P) GFP intensity of *UAS-5′ UTR^{Mical}-GFP* in c4da neurons expressing a control RNAi (O) or eIF3e RNAi (P).

(Q and R) GFP intensity of *UAS-GFP* in c4da neurons expressing a control RNAi (Q) or eIF3e RNAi (R).

(S) GFP intensities of *5′ UTR^{Mical}-GFP* reporters in (O) and (P).

(T) GFP intensities of regular *GFP* reporters in (Q) and (R).

(U) Reduction of GFP intensities of *UAS-5′ UTR^{Mical}-GFP* and *UAS-GFP* by eIF3e knockdown. Data are mean ± SEM. *$p < 0.05$, **$p < 0.005$, ***$p < 0.0005$, Wilcoxon test; n = 15–18. Scale bars, 10 μm.

See also Figures S5 and S6.

Mical 5′ UTR. To inhibit eIF4A pharmacologically, we used Rocaglamide A (RocA), a compound known to clamp eIF4A on the 5′ UTRs of target mRNAs (Iwasaki et al., 2016). S2 cells treated with 0.3 μM RocA for 10 min showed a decrease in translating ribosomes in polysome profiles (Figure 6B). We then used this condition to assess how eIF4A inhibition affects the interactions between eIF3 and 5′ UTR^{Mical} using an eIF3-RNA co-immunoprecipitation protocol (Gross et al., 2017). Here we transfected

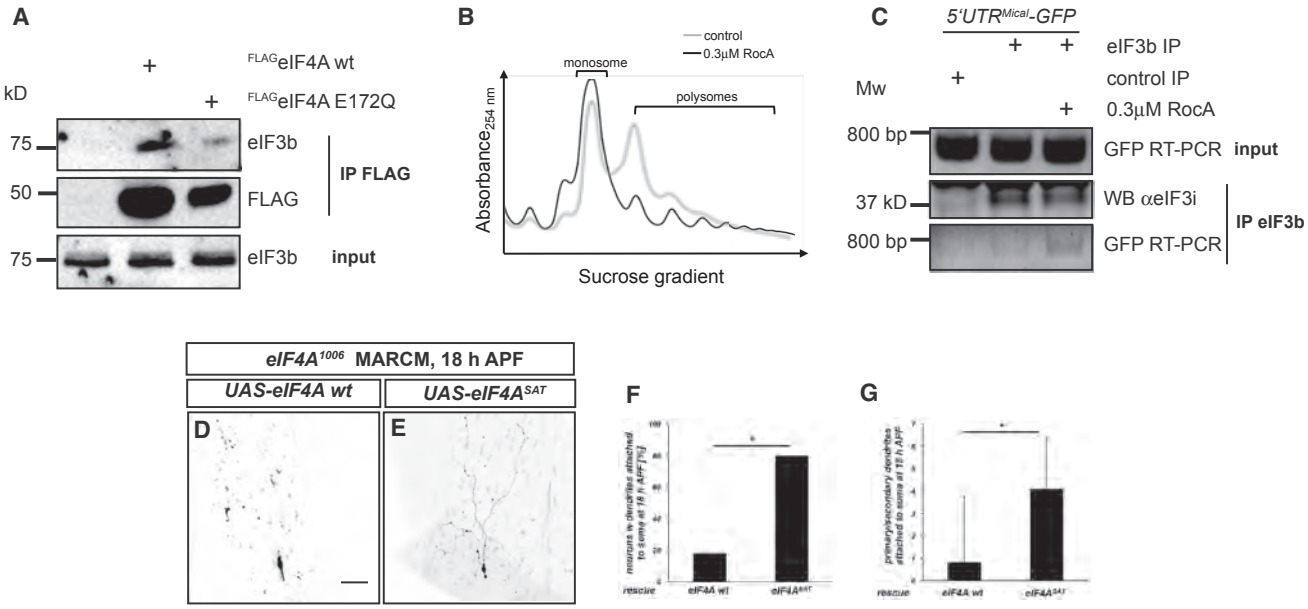

Figure 6. eIF4A Regulates Interactions between eIF3 and the Mical 5′ UTR

(A) eIF3 co-immunoprecipitates with eFLAG-tagged eIF4A in an ATPase-dependent manner. FLAG-tagged wild-type (WT) or ATPase-dead eIF4A constructs were transfected in S2R+ cells and precipitated with FLAG agarose. Precipitates were probed with anti-FLAG and anti-eIF3b antibodies. Molecular weight (MW) is indicated in kilodaltons (kDa).

(B) eIF4A inhibition with RocA leads to loss of translating ribosomes. Polysome profiles from control S2R+ cells (black line) or S2R+ cells treated with 0.3 μM RocA for 10 min are shown.

(C) eIF4A regulates interactions between eIF3 and a *5′ UTR^{Mical}* reporter mRNA. Control or anti-eIF3b immunoprecipitates from S2R+ cells expressing *5′ UTR^{Mical}-GFP* were analyzed by semiquantitative GFP RT-PCR. A 10-min treatment with 0.3 μM RocA results in increased eIF3b/*5′ UTR^{Mical}-GFP* interaction (n = 3).

(D–G) Requirement for eIF4A helicase activity during dendrite pruning. Wild-type eIF4A or helicase-dead were expressed in *eIF4A^{1006}* mutant MARCM clones, and the effects on c4da neuron dendrite pruning were assessed at 18 hr APF.

(D) Wild-type eIF4A rescues the pruning defects of *eIF4A^{1006}* c4da neuron MARCM clones at 18 hr APF (n = 10).

(E) Helicase-dead eIF4A^{SAT} does not rescue the pruning defects of *eIF4A^{1006}* mutant c4da neuron MARCM clones (n = 11).

(F) Penetrance of dendrite-pruning defects in (D) and (E). *p < 0.05, Fisher's exact test.

(G) Severity of dendrite-pruning defects in (D) and (E). *p < 0.05, Wilcoxon test. Data are mean ± SD.

See also Figure S7.

S2 cells with a *5′ UTR^{Mical}-GFP* reporter plasmid, then immunoprecipitated eIF3, and determined the amount of bound reporter mRNA by GFP RT-PCR. GFP mRNA could be detected in eIF3b precipitates from untreated cells, supporting the notion that eIF3 binds to the *5′ UTR^{Mical}-GFP* reporter also in S2 cells (Figure 6C). In samples treated with RocA, the GFP mRNA signal was increased at least 3-fold (n = 3; Figure 6C). This suggests that eIF4A activity is required for scanning of eIF3-dependent PICs on Mical mRNA.

The above result indicated that eIF4A might regulate eIF3-mRNA interactions through its helicase. To test *in vivo* whether the eIF4A helicase is important for dendrite pruning, we generated a UAS transgene encoding eIF4A^{SAT}, an eIF4A mutant that still has an active ATPase but that lacks helicase activity (Pause and Sonenberg, 1992). While wild-type eIF4A efficiently rescued the c4da neuron dendrite-pruning defects conferred by the *eIF4A^{1006}* mutant (Figure 6D), eIF4A^{SAT} did not (Figures 6E–6G), indicating that the helicase activity of eIF4A is required for dendrite pruning. Taken together, we conclude that eIF4A regulates the interaction between eIF3 and Mical mRNA, likely in a helicase-dependent manner.

eIF4A and eIF3 Are Broadly Required for Neuronal Remodeling in the Pupal PNS

So far, we have shown that eIF4A and eIF3 are specifically required for c4 da neuron dendrite pruning. Here, translation of Mical mRNA stringently depends on eIF4A and eIF3, while Sox14 mRNA can be translated via an eIF3- or an eIF4E-dependent pathway. As previous data had shown that ecdysone induces 4E-BP activity in tissues as diverse as fat body and neurons (Colombani et al., 2005; Wong et al., 2013), we next asked how broadly eIF4A and eIF3 were required for ecdysone-dependent neuronal remodeling in the PNS.

Two other types of peripheral sensory neurons undergo neuronal remodeling during the pupal phase: c1da neurons prune their larval dendrites with a similar time course as c4da neurons, whereas c3da neurons undergo apoptosis in an ecdysone-dependent manner around 7 hr APF (Williams and Truman, 2005). The c1da neuron dendrite pruning requires Mical, but c3da neuron apoptosis does not (Kirilly et al., 2009).

We first asked whether eIF4A and eIF3 were required for ecdysone-induced apoptosis. At 18 hr APF, the dorsal c3da

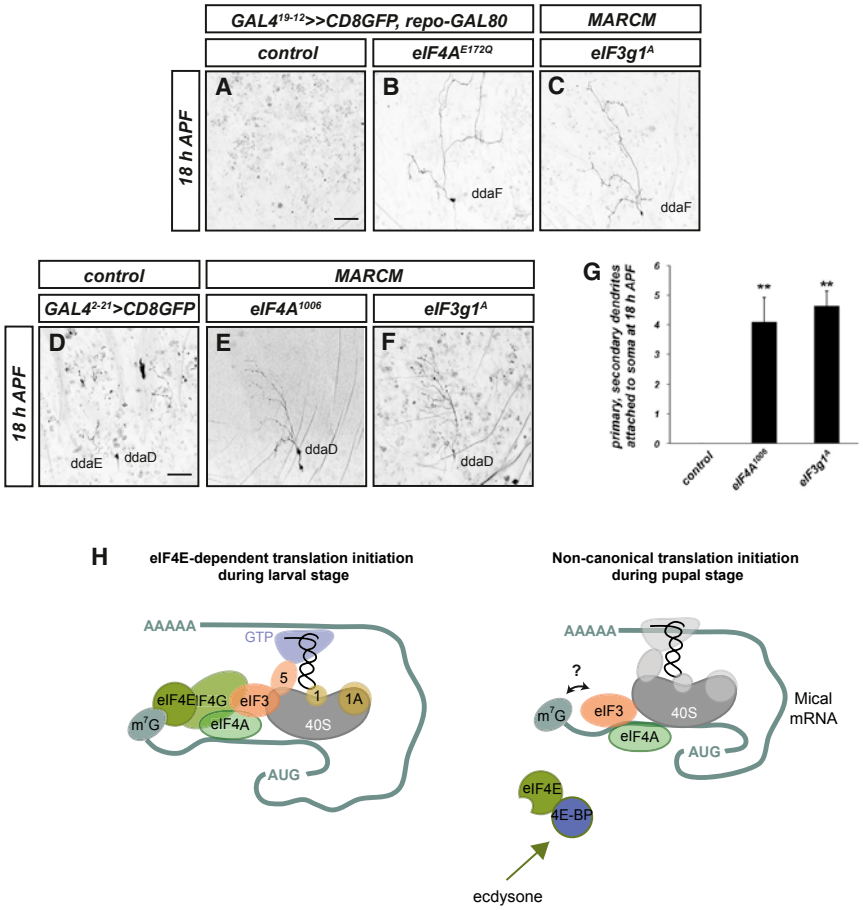

Figure 7. eIF4A/eIF3 Are Required Broadly for Ecdysone-Induced Neuronal Remodeling of Peripheral Sensory Neurons

(A–C) eIF4A and eIF3 are required for c3da neuron apoptosis. C3da neurons were labeled with the c3da neuron driver *GAL4*$^{19\text{-}12}$ or by MARCM and imaged at 18 hr APF. (A) Control c3da neurons labeled by *GAL4*$^{19\text{-}12}$ have undergone apoptosis (0/18 still detectable). (B) Expression of *eIF4A*^{E172Q} inhibits apoptosis in c3da neurons, mostly ddaF (18/48 still detectable). (C) A homozygous *eIF3g1*^{A} mutant c3da neuron failed to undergo apoptosis at 18 hr APF (n = 5).

(D–G) eIF4A and eIF3 are required for c1da neuron dendrite pruning. Pupae were imaged at 18 hr APF. (D) control c1 da neurons labeled with *GAL4*$^{2\text{-}21}$ have completely pruned their larval dendrites. (E and F) ddaD MARCM clones homozygous for *eIF4A*^{1006} (E) or *eIF3g1*^{A} (F) still possess long and branched dendrites at 18 hr APF. (G) Severity of c1 da neuron pruning defects in (D)–(F). Data are mean ± SD. **p < 0.005, Wilcoxon test; n = 6–11.

(H) Model for the regulation of translation initiation during c4 da neuron dendrite pruning. Cap recognition during the pupal stage is likely mediated by eIF3 (question mark in right panel). Scale bars, 50 μm.

neurons ddaA and ddaF had disappeared in control animals (Figure 7A). In contrast, expression of *eIF4A*^{E172Q} under a c3da-specific driver led to persistence of a fraction of c3da neurons, mainly ddaF, with intact processes until this stage (Figure 7B). Furthermore, we could detect homozygous *eIF3g1*^{A} mutant ddaF c3da neurons persisting at 18 hr APF (Figure 7C). Thus, eIF3 and eIF4A are required for c3da neuron apoptosis. Potential translation targets here could include pro-apoptotic factors, as *reaper* and *hid* mRNAs do not require eIF4E for translation (Hernández et al., 2004; Vazquez-Pianzola et al., 2007).

We next addressed the importance of eIF4A and eIF3 for c1da neuron dendrite pruning. In controls, ddaD c1da neuron dendrites were completely pruned at 18 hr APF (Figure 7D). In contrast, ddaD neurons lacking eIF4A or eIF3g1 (in *eIF4A*^{1006} or *eIF3g1*^{A} MARCM clones) still had long and branched dendrites attached to the cell body (Figures 7E–7G), indicating that eIF4A and eIF3 are also required for c1da neuron dendrite pruning. As c1da neuron dendrite pruning requires Mical (Kirilly et al., 2009), it is the most likely eIF4A/eIF3 target also during c1da neuron dendrite pruning. Taken together, our data indicate that eIF4A and eIF3 are part of a 4E-BP bypass system that is broadly required for ecdysone-induced neuronal remodeling in the *Drosophila* PNS.

DISCUSSION

Developmental control of translation rate is required under various conditions. One well-characterized regulatory mechanism is through 4E-BP, which inhibits assembly of the cap-binding eIF4F complex (Gingras et al., 1999). Despite the obvious need for global translation control during development, it is also clear that there must be exceptions to such regulation. Several lines of evidence suggest that global, eIF4E-dependent translation is downregulated by ecdysone during the pupal phase (Colombani et al., 2005; Hoopfer et al., 2008; Wong et al., 2013) and that this is important for c4da neuron dendrite pruning (Wong et al., 2013). How downregulation of eIF4E-dependent translation contributes to dendrite pruning is not clear. TOR activity (and hence eIF4E-dependent translation) is associated with neurite regrowth after pruning in a *Drosophila* model for neuronal remodeling (Yaniv et al., 2012), and beta-actin mRNA was identified as a 4E-BP target in vertebrate neurons (Leung et al., 2006). General suppression of eIF4E-dependent translation may, therefore, serve to prevent precocious neurite growth or neurite stabilization through increased actin polymerization.

Despite the need for translation downregulation during dendrite pruning, ecdysone-induced mRNAs must still be efficiently translated. We found that c4 da neuron dendrite pruning does not depend on the eIF4F subunits eIF4E and eIF4G, but instead on eIF3 and eIF4A (Figure 7H). In keeping with a specific effect on dendrite-pruning genes, we could identify Mical mRNA as the crucial target for eIF3 and eIF4A. Our data suggest that this specificity is encoded in the 5′ UTR of Mical mRNA, as a

UAS-GFP reporter containing the Mical 5′ UTR showed consistently stronger dependence on eIF4A and eIF3 than a regular UAS-GFP reporter (Figure 5). The important role of the Mical 5′ UTR is also supported by our observation that Sox14 overexpression (which induces endogenous Mical mRNA) did not rescue the pruning defects induced by eIF4A RNAi, while overexpression of Mical from a UAS transgene (and thus lacking the endogenous 5′ UTR) did (Figures 4, S4, and 5). It is tempting to speculate that eIF3-eIF4A recognition signals may be abundant in 5′ UTRs of ecdysone-induced genes.

Several lines of evidence indicate that translation initiation of pupal pruning factors in c4 da neurons is still cap dependent: for one, overexpression of a cap-binding-deficient eIF3d mutant causes dominant dendrite-pruning defects (Figure 2I), and *in vitro* translation of a 5′ UTR^{Mical} reporter mRNA depends on a functional cap (Figure S5). While we observed physical interactions between eIF3 and a 5′ UTR^{Mical} reporter mRNA in S2 cells, we could not directly demonstrate cap binding by eIF3 *in vivo*. eIF3 does not bind to the isolated cap structure (Lee et al., 2016; Figure S7), and a biochemical cap-binding assay for eIF3 would require crosslinking eIF3 with a purified mRNA with a radioactively labeled cap. To further investigate developmental control of translation initiation in the future, it would be interesting to set up such an assay to address whether the Mical mRNA cap is also recognized via eIF3d or another eIF3 subunit.

Sox14 expression seemed resistant to the inhibition of either eIF4E or eIF3, but we found that these pathways can mediate Sox14 expression in a redundant fashion. Sox14 is upstream of the Cul-1 ubiquitin ligase that activates 4E-BP in c4da neurons (Wong et al., 2013). Its mRNA may be adapted to this position in the pruning pathway, as it could still use the regular eIF4F pathway early during the pupal phase and the eIF3 pathway later. Mical translation may only start when 4E-BP activity is already high, hence explaining its strong eIF3 dependence.

Translation of long mRNAs is sensitive to the eIF4A cofactor eIF4B (Sen et al., 2016), and eIF4A dependence is also in part conferred by sequences in the coding region (Yourik et al., 2017). eIF4B manipulation did not cause dendrite pruning defects (Figure S1), but the Mical construct used to rescue the pruning defects induced by eIF4A knockdown lacks an internal region non-essential for pruning (Kirilly et al., 2009). It is, therefore, possible that internal regions of the long Mical mRNA also contribute to its dependence on eIF4A.

The strong similarities between the phenotypes caused by the manipulation of eIF4A and eIF3 suggested that these two factors cooperate functionally. We found that eIF4A and eIF3 can be found in an eIF4A ATPase-dependent complex and that eIF4A clamping on the mRNA prevents eIF3 release from a 5′ UTR^{Mical} reporter mRNA (Figure 6). Two recent *in vitro* studies found functional interactions between eIF4A and eIF3 in the context of canonical eIF4F-dependent translation initiation (Yourik et al., 2017; Sokabe and Fraser, 2017): first, eIF3 stimulates eIF4A ATPase activity via its eIF3g subunit to promote PIC maturation (Yourik et al., 2017); and, second, eIF4A ATPase activity was required to reposition the eIF3j subunit within the PIC during maturation (Sokabe and Fraser, 2017). We now demonstrate genetically that eIF4A has an eIF3-related function independently of eIF4F. Our data showing that eIF3 and eIF4A interact in an ATPase-dependent manner and that eIF4A helicase activity is required for dendrite pruning are consistent with both the above proposals.

Taken together, our data suggest that eIF3-eIF4A are part of a bypass mechanism that ensures translation of crucial ecdysone-induced mRNAs in the absence of an eIF4E-dependent translation initiation during developmental neuronal remodeling in the *Drosophila* PNS.

STAR★METHODS

Detailed methods are provided in the online version of this paper and include the following:

- KEY RESOURCES TABLE
- CONTACT FOR REAGENT AND RESOURCE SHARING
- EXPERIMENTAL MODEL AND SUBJECT DETAILS
  - Fly Strains
- METHOD DETAILS
  - Cloning and transgenes
  - Dissection, Microscopy and Live imaging
  - 5′UTR^{Mical}-GFP reporter
  - Fluorescent Nonanonical Amino Acid Tagging
  - Antibodies and immunohistochemistry
  - *In vitro* transcription and translation
  - Immunoprecipitations and affinity pulldown
  - Polysome profile
- QUANTIFICATION AND STATISTICAL ANALYSIS
  - Imaging analysis

SUPPLEMENTAL INFORMATION

Supplemental Information includes seven figures and one table and can be found with this article online at https://doi.org/10.1016/j.celrep.2018.07.074.

ACKNOWLEDGMENTS

We are grateful to C. Klämbt for generous support and to C. Klämbt, R. Stanewsky, and Rumpf lab members for helpful comments on the manuscript. We are indebted to M. Hentze; M. Somma; M. Marr; C. Klämbt; Y. Jan; B. Edgar; A. Kolodkin; J. Terman; and the DSHB, Bloomington, VDRC, and Kyoto stock centers for fly stocks and reagents. We would like to thank C. Meignin for advice on biochemical experiments; O. Schuldiner for discussions; L. Garcia for help with statistics; J. Bussmann for help with FUNCAT; and A. McNally, A. Althoff, S. Schindler, and A. Fleige for help with experiments. This research was funded by the DFG Excellence cluster EXC 1003 "Cells in Motion" (junior group S. Rumpf, CiM grant FF-2016-13 to S. Rumpf and A.R., and CiM grant PP-2016-20 to O.S. and S. Rode).

AUTHOR CONTRIBUTIONS

S. Rode and S. Rumpf designed and conceived the project and interpreted the data. S. Rode, M.R., and S. Rumpf contributed reagents. S. Rode, H.O., L.A., M.W., X.D., O.S., and S. Rumpf performed experiments and interpreted data. S. Rumpf wrote the manuscript with input from S. Rode, E.S., S.A.L., A.R., and S.Z.

DECLARATION OF INTERESTS

The authors declare no competing interests.

Received: October 13, 2017
Revised: June 22, 2018
Accepted: July 23, 2018
Published: August 28, 2018

REFERENCES

Cate, J.H. (2017). Human eIF3: from "blobology" to biological insight. Philos. Trans. R. Soc. Lond. B Biol. Sci. *372*, 20160176.

Colombani, J., Bianchini, L., Layalle, S., Pondeville, E., Dauphin-Villemant, C., Antoniewski, C., Carré, C., Noselli, S., and Léopold, P. (2005). Antagonistic actions of ecdysone and insulins determine final size in Drosophila. Science *310*, 667–670.

Dietzl, G., Chen, D., Schnorrer, F., Su, K.-C., Barinova, Y., Fellner, M., Gasser, B., Kinsey, K., Oppel, S., Scheiblauer, S., et al. (2007). A genome-wide transgenic RNAi library for conditional gene inactivation in Drosophila. Nature *448*, 151–156.

Erdmann, I., Marter, K., Kobler, O., Niehues, S., Abele, J., Müller, A., Bussmann, J., Storkebaum, E., Ziv, T., Thomas, U., and Dieterich, D.C. (2015). Cell-selective labelling of proteomes in Drosophila melanogaster. Nat. Commun. *6*, 7521.

Galloni, M., and Edgar, B.A. (1999). Cell-autonomous and non-autonomous growth-defective mutants of Drosophila melanogaster. Development *126*, 2365–2375.

Gandin, V., Masvidal, L., Hulea, L., Gravel, S.-P., Cargnello, M., McLaughlan, S., Cai, Y., Balanathan, P., Morita, M., Rajakumar, A., et al. (2016). nanoCAGE reveals 5′ UTR features that define specific modes of translation of functionally related MTOR-sensitive mRNAs. Genome Res. *26*, 636–648.

Gingras, A.C., Raught, B., and Sonenberg, N. (1999). eIF4 initiation factors: effectors of mRNA recruitment to ribosomes and regulators of translation. Annu. Rev. Biochem. *68*, 913–963.

Gross, L., Vicens, Q., Einhorn, E., Noireterre, A., Schaeffer, L., Kuhn, L., Imler, J.-L., Eriani, G., Meignin, C., and Martin, F. (2017). The IRES5'UTR of the dicistrovirus cricket paralysis virus is a type III IRES containing an essential pseudoknot structure. Nucleic Acids Res. *45*, 8993–9004.

Grueber, W.B., Ye, B., Yang, C.-H., Younger, S., Borden, K., Jan, L.Y., and Jan, Y.-N. (2007). Projections of Drosophila multidendritic neurons in the central nervous system: links with peripheral dendrite morphology. Development *134*, 55–64.

Han, C., Song, Y., Xiao, H., Wang, D., Franc, N.C., Jan, L.Y., and Jan, Y.-N. (2014). Epidermal cells are the primary phagocytes in the fragmentation and clearance of degenerating dendrites in Drosophila. Neuron *81*, 544–560.

Hernández, G., Vázquez-Pianzola, P., Sierra, J.M., and Rivera-Pomar, R. (2004). Internal ribosome entry site drives cap-independent translation of reaper and heat shock protein 70 mRNAs in Drosophila embryos. RNA *10*, 1783–1797.

Herzmann, S., Krumkamp, R., Rode, S., Kintrup, C., and Rumpf, S. (2017). PAR-1 promotes microtubule breakdown during dendrite pruning in *Drosophila*. EMBO J. *36*, 1981–1991.

Herzmann, S., Götzelmann, I., Reekers, L.-F., and Rumpf, S. (2018). Spatial regulation of microtubule disruption during dendrite pruning in *Drosophila*. Development *145*, dev156950.

Hinnebusch, A.G. (2014). The scanning mechanism of eukaryotic translation initiation. Annu. Rev. Biochem. *83*, 779–812.

Holstein, J.M., Anhäuser, L., and Rentmeister, A. (2016). Modifying the 5′-Cap for Click Reactions of Eukaryotic mRNA and To Tune Translation Efficiency in Living Cells. Angew. Chem. Int. Ed. Engl. *55*, 10899–10903.

Hoopfer, E.D., Penton, A., Watts, R.J., and Luo, L. (2008). Genomic analysis of Drosophila neuronal remodeling: a role for the RNA-binding protein Boule as a negative regulator of axon pruning. J. Neurosci. *28*, 6092–6103.

Hsieh, A.C., Liu, Y., Edlind, M.P., Ingolia, N.T., Janes, M.R., Sher, A., Shi, E.Y., Stumpf, C.R., Christensen, C., Bonham, M.J., et al. (2012). The translational landscape of mTOR signalling steers cancer initiation and metastasis. Nature *485*, 55–61.

Hung, R.-J., Yazdani, U., Yoon, J., Wu, H., Yang, T., Gupta, N., Huang, Z., van Berkel, W.J.H., and Terman, J.R. (2010). Mical links semaphorins to F-actin disassembly. Nature *463*, 823–827.

Iwasaki, S., Floor, S.N., and Ingolia, N.T. (2016). Rocaglates convert DEAD-box protein eIF4A into a sequence-selective translational repressor. Nature *534*, 558–561.

Kirilly, D., Gu, Y., Huang, Y., Wu, Z., Bashirullah, A., Low, B.C., Kolodkin, A.L., Wang, H., and Yu, F. (2009). A genetic pathway composed of Sox14 and Mical governs severing of dendrites during pruning. Nat. Neurosci. *12*, 1497–1505.

Kumar, P., Hellen, C.U.T., and Pestova, T.V. (2016). Toward the mechanism of eIF4F-mediated ribosomal attachment to mammalian capped mRNAs. Genes Dev. *30*, 1573–1588.

Kuo, C.T., Jan, L.Y., and Jan, Y.N. (2005). Dendrite-specific remodeling of Drosophila sensory neurons requires matrix metalloproteases, ubiquitin-proteasome, and ecdysone signaling. Proc. Natl. Acad. Sci. USA *102*, 15230–15235.

Lachance, P.E.D., Miron, M., Raught, B., Sonenberg, N., and Lasko, P. (2002). Phosphorylation of eukaryotic translation initiation factor 4E is critical for growth. Mol. Cell. Biol. *22*, 1656–1663.

Lee, T., and Luo, L. (1999). Mosaic analysis with a repressible cell marker for studies of gene function in neuronal morphogenesis. Neuron *22*, 451–461.

Lee, A.S.Y., Kranzusch, P.J., and Cate, J.H.D. (2015). eIF3 targets cell-proliferation messenger RNAs for translational activation or repression. Nature *522*, 111–114.

Lee, A.S., Kranzusch, P.J., Doudna, J.A., and Cate, J.H.D. (2016). eIF3d is an mRNA cap-binding protein that is required for specialized translation initiation. Nature *536*, 96–99.

Leung, K.-M., van Horck, F.P.G., Lin, A.C., Allison, R., Standart, N., and Holt, C.E. (2006). Asymmetrical beta-actin mRNA translation in growth cones mediates attractive turning to netrin-1. Nat. Neurosci. *9*, 1247–1256.

Loncle, N., and Williams, D.W. (2012). An interaction screen identifies headcase as a regulator of large-scale pruning. J. Neurosci. *32*, 17086–17096.

Luo, L., and O'Leary, D.D.M. (2005). Axon retraction and degeneration in development and disease. Annu. Rev. Neurosci. *28*, 127–156.

Matsubara, D., Horiuchi, S.-Y., Shimono, K., Usui, T., and Uemura, T. (2011). The seven-pass transmembrane cadherin Flamingo controls dendritic self-avoidance via its binding to a LIM domain protein, Espinas, in Drosophila sensory neurons. Genes Dev. *25*, 1982–1996.

Meyer, K.D., Patil, D.P., Zhou, J., Zinoviev, A., Skabkin, M.A., Elemento, O., Pestova, T.V., Qian, S.-B., and Jaffrey, S.R. (2015). 5′ UTR m(6)A Promotes Cap-Independent Translation. Cell *163*, 999–1010.

Miron, M., Verdú, J., Lachance, P.E., Birnbaum, M.J., Lasko, P.F., and Sonenberg, N. (2001). The translational inhibitor 4E-BP is an effector of PI(3)K/Akt signalling and cell growth in Drosophila. Nat. Cell Biol. *3*, 596–601.

Niehues, S., Bussmann, J., Steffes, G., Erdmann, I., Köhrer, C., Sun, L., Wagner, M., Schäfer, K., Wang, G., Koerdt, S.N., et al. (2015). Impaired protein translation in Drosophila models for Charcot-Marie-Tooth neuropathy caused by mutant tRNA synthetases. Nat. Commun. *6*, 7520.

Olson, C.M., Donovan, M.R., Spellberg, M.J., and Marr, M.T., 2nd. (2013). The insulin receptor cellular IRES confers resistance to eIF4A inhibition. eLife *2*, e00542.

Osterwalder, T., Yoon, K.S., White, B.H., and Keshishian, H. (2001). A conditional tissue-specific transgene expression system using inducible GAL4. Proc. Natl. Acad. Sci. USA *98*, 12596–12601.

Pause, A., and Sonenberg, N. (1992). Mutational analysis of a DEAD box RNA helicase: the mammalian translation initiation factor eIF-4A. EMBO J. *11*, 2643–2654.

Pfeiffer, B.D., Jenett, A., Hammonds, A.S., Ngo, T.-T.B., Misra, S., Murphy, C., Scully, A., Carlson, J.W., Wan, K.H., Laverty, T.R., et al. (2008). Tools for

neuroanatomy and neurogenetics in Drosophila. Proc. Natl. Acad. Sci. USA *105*, 9715–9720.

Renda, F., Pellacani, C., Strunov, A., Bucciarelli, E., Naim, V., Bosso, G., Kiseleva, E., Bonaccorsi, S., Sharp, D.J., Khodjakov, A., et al. (2017). The Drosophila orthologue of the INT6 onco-protein regulates mitotic microtubule growth and kinetochore structure. PLoS Genet. *13*, e1006784.

Richter, J.D., and Sonenberg, N. (2005). Regulation of cap-dependent translation by eIF4E inhibitory proteins. Nature *433*, 477–480.

Ritter, A.R., and Beckstead, R.B. (2010). Sox14 is required for transcriptional and developmental responses to 20-hydroxyecdysone at the onset of drosophila metamorphosis. Dev. Dyn. *239*, 2685–2694.

Rumpf, S., Lee, S.B., Jan, L.Y., and Jan, Y.N. (2011). Neuronal remodeling and apoptosis require VCP-dependent degradation of the apoptosis inhibitor DIAP1. Development *138*, 1153–1160.

Rumpf, S., Bagley, J.A., Thompson-Peer, K.L., Zhu, S., Gorczyca, D., Beckstead, R.B., Jan, L.Y., and Jan, Y.N. (2014). Drosophila Valosin-Containing Protein is required for dendrite pruning through a regulatory role in mRNA metabolism. Proc. Natl. Acad. Sci. USA *111*, 7331–7336.

Schuldiner, O., and Yaron, A. (2015). Mechanisms of developmental neurite pruning. Cell. Mol. Life Sci. *72*, 101–119.

Sen, N.D., Zhou, F., Harris, M.S., Ingolia, N.T., and Hinnebusch, A.G. (2016). eIF4B stimulates translation of long mRNAs with structured 5′ UTRs and low closed-loop potential but weak dependence on eIF4G. Proc. Natl. Acad. Sci. USA *113*, 10464–10472.

Sokabe, M., and Fraser, C.S. (2017). A helicase-independent activity of eIF4A in promoting mRNA recruitment to the human ribosome. Proc. Natl. Acad. Sci. USA *114*, 6304–6309.

Svitkin, Y.V., Pause, A., Haghighat, A., Pyronnet, S., Witherell, G., Belsham, G.J., and Sonenberg, N. (2001). The requirement for eukaryotic initiation factor 4A (eIF4A) in translation is in direct proportion to the degree of mRNA 5′ secondary structure. RNA *7*, 382–394.

Terman, J.R., Mao, T., Pasterkamp, R.J., Yu, H.-H., and Kolodkin, A.L. (2002). MICALs, a family of conserved flavoprotein oxidoreductases, function in plexin-mediated axonal repulsion. Cell *109*, 887–900.

Vazquez-Pianzola, P., Hernández, G., Suter, B., and Rivera-Pomar, R. (2007). Different modes of translation for hid, grim and sickle mRNAs in Drosophila. Cell Death Differ. *14*, 286–295.

Williams, D.W., and Truman, J.W. (2005). Cellular mechanisms of dendrite pruning in Drosophila: insights from in vivo time-lapse of remodeling dendritic arborizing sensory neurons. Development *132*, 3631–3642.

Wolfe, A.L., Singh, K., Zhong, Y., Drewe, P., Rajasekhar, V.K., Sanghvi, V.R., Mavrakis, K.J., Jiang, M., Roderick, J.E., Van der Meulen, J., et al. (2014). RNA G-quadruplexes cause eIF4A-dependent oncogene translation in cancer. Nature *513*, 65–70.

Wong, J.J.L., Li, S., Lim, E.K.H., Wang, Y., Wang, C., Zhang, H., Kirilly, D., Wu, C., Liou, Y.-C., Wang, H., and Yu, F. (2013). A Cullin1-based SCF E3 ubiquitin ligase targets the InR/PI3K/TOR pathway to regulate neuronal pruning. PLoS Biol. *11*, e1001657.

Xiang, Y., Yuan, Q., Vogt, N., Looger, L.L., Jan, L.Y., and Jan, Y.N. (2010). Light-avoidance-mediating photoreceptors tile the Drosophila larval body wall. Nature *468*, 921–926.

Yamamoto, H., Unbehaun, A., and Spahn, C.M.T. (2017). Ribosomal Chamber Music: Toward an Understanding of IRES Mechanisms. Trends Biochem. Sci. *42*, 655–668.

Yaniv, S.P., Issman-Zecharya, N., Oren-Suissa, M., Podbilewicz, B., and Schuldiner, O. (2012). Axon regrowth during development and regeneration following injury share molecular mechanisms. Curr. Biol. *22*, 1774–1782.

Yourik, P., Aitken, C.E., Zhou, F., Gupta, N., Hinnebusch, A.G., and Lorsch, J.R. (2017). Yeast eIF4A enhances recruitment of mRNAs regardless of their structural complexity. eLife *6*, e31476.

STAR★METHODS

KEY RESOURCES TABLE

REAGENT or RESOURCE	SOURCE	IDENTIFIER
Antibodies		
chicken anti-GFP	Aves lab	cat. # GFP-1020; RRID: AB_10000240
mouse anti-GFP 3E6	Invitrogen	cat. # A-11120; RRID: AB_2313858
rat anti-cherry 16D7	Invitrogen	cat. # M11217
mouse anti-FLAG M2	Sigma	cat. # F1804; RRID: AB_262044
mouse anti-EcR	DSHB	Ag10.2; RRID: AB_528208
mouse anti-hdc	DSHB	U33; RRID: AB_10659722
guinea pig anti-Sox14	gift from R. Beckstead	(Ritter and Beckstead, 2010)
rabbit anti-Mical	this study	N/A
rabbit anti-eIF4A	gift from M. Marr	(Olson et al., 2013)
rabbit anti-eIF3e	gift from M. Somma	(Renda et al., 2017)
rabbit anti-eIF3b	gift from M. Hentze	N/A
rabbit anti-eIF3i	gift from M. Hentze	N/A
rabbit anti-eIF3j	gift from M. Hentze	N/A
anti-FLAG affinity resin	Sigma	cat. # A2220
rabbit anti-DsRed	Clontech	cat. # 632496; RRID:_AB10013483
Chemicals, Peptides, and Recombinant Proteins		
Rocaglamide A	Santa Cruz Biotechnology	cat. # 203241
20-hydroxyecdysone	Sigma	cat. # H5142
RU486	Sigma	cat. # M8046
Trizol Reagent	Invitrogen	cat. # 15596026
$m_2^{7,3'}$-OGpppG (ARCA) cap analog	Jena Bioscience	cat. # NU-855S
ApppG cap analog	NEB	cat. # S1406L
γ-Aminophenyl-m7GTP (C10-spacer)-Agarose	Jena Bioscience	cat. # AC-155S
Dynabeads Protein G	Invitrogen	cat. # 10003D
Critical Commercial Assays		
Superscript-III Reverse Transcriptase	Invitrogen	Cat. No. 18080400
Retic Lysate IVT™ Kit	Invitrogen	cat. # AM1200
Gaussia-Juice Luciferase Assay Kit	pjk GmbH	cat. # 102540
FuGENE transfection reagent	Promega	cat. # E2311
Experimental Models: Cell Lines		
D. melanogaster: Cell line S2: S2R+	gift from S. Bogdan	N/A
Experimental Models: Organisms/Strains		
Drosophila melanogaster w^{1118}	N/A	N/A
ppk-GAL4 (II)	gift from Y. Jan	(Grueber et al., 2007)
ppk-GAL4 (III)	gift from Y. Jan	(Grueber et al., 2007)
ppk-GS	gift from R. Yang	N/A
ppk-CD4::tdtomato	gift from C. Han	N/A
UAS-mCD8GFP	Bloomington	(Lee and Luo, 1999)
UAS-tdtomato	gift from C. Han	(Han et al., 2014)
UAS-dcr2	VDRC	(Dietzl et al., 2007)
$GAL4^{109(2)80}$	gift from Y. Jan	N/A
$GAL4^{R57C10}$	Bloomington	(Pfeiffer et al., 2008)
$GAL4^{19-12}$	gift from Y. Jan	N/A

(*Continued on next page*)

Continued

REAGENT or RESOURCE	SOURCE	IDENTIFIER
$GAL4^{2-21}$	gift from Y. Jan	N/A
SOP-FLP	gift from T. Uemura	(Matsubara et al., 2011)
UAS-4E-BP LL	Bloomington	BDSC 24854
UAS-GFP	Bloomington	BDSC 5431
UAS-eIF4A wt	this study	N/A
UAS-eIF4A E172Q	this study	N/A
UAS-$eIF4A^{SAT}$	this study	N/A
UAS-eIF3d wt	FlyORF collection	FlyORF F001520
UAS-$eIF3d^{helix11}$	this study	N/A
UAS-5′UTR-^{Mical}GFP	this study	N/A
UAS-Mical	gift from A. Kolodkin	(Terman et al., 2002)
UAS-MicalΔC	gift from A. Kolodkin	(Terman et al., 2002)
UAS-GFP::Mical	gift from J. Terman	(Hung et al., 2010)
UAS-GFP::MicalΔCH	gift from J. Terman	(Hung et al., 2010)
UAS-GFP::MicalΔRedox	gift from J. Terman	(Hung et al., 2010)
UAS-Sox14	Rumpf lab	(Rumpf et al., 2014)
UAS-$dMetRS^{L262G}$	gift from D. Dieterich	(Erdmann et al., 2015)
UAS-lacZ	Bloomington	(BDSC 1777)
P[lacW]eIF4A^{1006}, FRT40A	gift from B. Edgar	(Galloni and Edgar, 1999)
eIF4E^{s058911}, FRT2A	this study/Bloomington	BDSC 8648
FRT42D, eIF3b^{EY14430}	DRGC	Kyoto 114685
eIF3g1^{A}, FRT19A	Bloomington	BDSC 52344
UAS-eIF4E RNAi	Bloomington	BDSC 34096
UAS-eIF4E RNAi	VDRC	VDRC 7800
UAS-eIF4G1 RNAi	VDRC	VDRC 17003
UAS-eIF4G1 RNAi	Bloomington	BDSC 33049
UAS-eIF4B RNAi	VDRC	VDRC 31364
UAS-eIF4B RNAi	Bloomington	BDSC 57305
UAS-eIF4A RNAi	VDRC	VDRC 42202
UAS-eIF4A RNAi	VDRC	VDRC 42201
UAS-eIF4A RNAi	Bloomington	BDSC 32970
UAS-eIF3c RNAi	VDRC	VDRC 26667
UAS-eIF3e RNAi	VDRC	VDRC 27032
UAS-cherry RNAi	Bloomington	BDSC 35785
UAS-Orco RNAi	Bloomington	BDSC 31278
Oligonucleotides		
Ggacggatccaagatgagtaaaggagaagaacttttcac fw primer for GFP RT-PCR	this study	N/A
rev primer for GFP RT-PCR	this study	N/A
Recombinant DNA		
pUAST attB-^{FLAG}eIF4A wt	this study	N/A
pUAST attB-^{FLAG}eIF4A E172Q	this study	N/A
pUAST attB-5′UTR^{Mical}-GFP	this study	N/A
Act5C-GAL4	gift from S. Bogdan	N/A
pBS SK(-)5′UTR^{Mical}-RLuc	this study	N/A
pMRNA mRNAExpress-RLuc	Rentmeister lab	(Holstein et al., 2016)
pGEX4T-1 MicalC245 for recombinant protein and antibody production	this study	N/A
Software and Algorithms		
Fiji	NIH	https://fiji.sc/
Graphpad Prism	Graphpad Software	https://www.graphpad.com/

CONTACT FOR REAGENT AND RESOURCE SHARING

Detailed information and requests for resources generated in this paper should be directed to Sebastian Rumpf (sebastian.rumpf@uni-muenster.de).

EXPERIMENTAL MODEL AND SUBJECT DETAILS

Fly Strains

All strains and crosses were kept at 25°C under standard conditions. For expression in c4 da neurons, we used *ppk-GAL4* insertions on the second and third chromosomes or *ppk-GeneSwitch* (Grueber et al., 2007; Rumpf et al., 2011). C3 da neurons were labeled by $GAL4^{19\text{-}12}$ (Xiang et al., 2010), and c1 da neurons with $GAL4^{2\text{-}21}$. MARCM clones were induced with *SOP-FLP* (Matsubara et al., 2011) and labeled by tdtomato expression under $nsyb\text{-}GAL4^{R57C10}$ or mCD8GFP expression under $GAL4^{109(2)80}$. Mutant alleles used for MARCM were (1) $eIF4E1^{s058911}$, *FRT2A*, (2) $P[lacW]eIF4A^{1006}$, *FRT40A* (Galloni and Edgar, 1999), (3) *FRT42D*, $eIF3b^{EY14430}$ (Kyoto #114685) and (4) $eIF3g1^{A}$, FRT19A (BL # 52344). Other fly lines were UAS-Mical, UAS-MicalΔC (Terman et al., 2002), UAS-GFP::Mical, UAS-GFP::MicalΔCH, UAS-GFP::MicalΔRedox (Hung et al., 2010), UAS-Sox14 (Rumpf et al., 2014), UAS-tdtomato (Han et al., 2014), UAS-GFP (BL #5431), UAS-4E-BP LL (Miron et al., 2001). UAS-RNAi lines were: *eIF4E1* (BL #34096, VDRC 7800), *eIF4G1* (VDRC 17003, BL #33049), *eIF4B* (VDRC 31364, BL #57305), *eIF4A* (#1, VDRC 42202, #2, VDRC 42201, #3, BL #32970), *eIF3c* (VDRC 26667), *eIF3e* (VDRC 27032). UAS-cherry RNAi (BL #35785) or UAS-Orco RNAi (BL #31278) were used as controls. UAS-RNAi lines were used with UAS-dcr2 (Dietzl et al., 2007). UAS-$dMetRS^{L262G}$ was used for fluorescent noncanonical amino acid tagging (FUNCAT) (Erdmann et al., 2015).

METHOD DETAILS

Cloning and transgenes

$eIF4A^{E172Q}$, $eIF4A^{SAT}$ and $5'UTR^{Mical}$-*GFP* were cloned into pUAST attB by standard methods, and point mutations were introduced by Quikchange mutagenesis. Transgenes were injected in flies carrying VK37 or attP2 acceptor sites.

Dissection, Microscopy and Live imaging

For analysis of pruning defects, pupae were dissected out of the pupal case at 18 h APF and analyzed live using a Zeiss LSM710 confocal microscope. For *eIF4A* genetic interactions, candidates were crossed to a second chromosome insertion of *ppk-GAL4* combined with UAS-CD8GFP and *UAS-eIF4A RNAi* #1 (VDRC 42202).

$5'UTR^{Mical}$-GFP reporter

Reporter lines were established with *UAS-GFP*, and *UAS-*$5'UTR^{Mical}$*-GFP* on the second chromosome and *ppk-GAL4*, *UAS-tdtomato* on the third. These lines were then crossed to *UAS-4E-BP LL* (and *UAS-lacZ* as control) or *UAS-dcr2*; *UAS-eIF4A RNAi#1* and *UAS-dcr2*; *UAS-eIF3e RNAi* lines, respectively (and *UAS-dcr2*; *UAS-Orco RNAi* as control).

Fluorescent Nonanonical Amino Acid Tagging

Translation rate measurements in c4 da neurons were done as described (Niehues et al., 2015). Briefly, larvae were kept on food containing 4 mM ANL for 48 h. Click chemistry with TAMRA dye was performed after dissection and fixation in 4% formaldehyde.

Antibodies and immunohistochemistry

Pupal body wall filets were dissected quickly in PBS and fixed in PBS containing 4% formaldehyde for 20 minutes. Mouse, or chicken anti-GFP antibodies were from Life technologies or Aves labs, respectively, rabbit anti-DsRed from Clontech, and rat anti-mcherry from Life technologies. Other antibodies were mouse anti-HDC U33 (DSHB), mouse anti-EcR Ag10.2 (DSHB), guinea pig anti-Sox14 (Ritter and Beckstead, 2010). Rabbit anti-Mical antibodies were raised against a recombinantly expressed GST-tagged fragment corresponding to the C-terminal 245 amino acids of Mical.

In vitro transcription and translation

For the production of *Renilla* luciferase (RLuc) mRNAs, the following plasmids were used: $pMRNA^{xp}$ *mRNAExpress-RLuc* (Holstein et al., 2016) (for production of a cap-dependent control mRNA) and pBS KS(-)T7-5′-UTR^{Mical}-RLuc (for analysis of cap-dependence of the Mical 5′-UTR). *In vitro* T7 transcription was performed in 25 μL scale in 1x transcription buffer (200 mM Tris-HCl (pH 7.9), 30 mM $MgCl_2$, 50 mM DTT, 50 mM NaCl, 10 mM spermidine using 100 ng DNA template (linearized plasmid), 1 mM ARCA or ApppG cap analog, 30 U RiboLock RNase Inhibitor, 50 U T7 RNA polymerase and 0.1 U pyrophosphatase for 3 h at 37°C. DNA templates were digested by with 2 U DNase I for 1 h at 37°C and mRNAs were purified using the RNA Clean & Concentrator™-5 Kit (*Zymo Research*). Digestion of non-capped ppp-RNAs were performed in 20 μL scale in 1x reaction puffer (*epicenter*) using 2.5 μg purified mRNA and 20 U RNA 5′ polyphosphatase for 30 min at 37°C. Immediately after the incubation, 5 mM $MgCl_2$ and 1 U XRN-1 were added, and the reaction mixture was incubated at 37°C for 1 h. The capped mRNAs were purified using the RNA Clean & Concentrator™-5 Kit (*Zymo Research*).

RNA purity and integrity was confirmed by RNA gel analysis using 7.5% denatured polyacrylamide gel (25% acrylamide/bisacrylamide 19:1 and 50% urea).

In vitro translation was performed using the Retic Lysate IVT™ Kit (*Invitrogen*). 0, 6.25, 12.5, 25 and 37.5 ng mRNA were incubated with 8.5 μL rabbit reticulocyte lysate, 0.05 mM L-methionine and 1x translation mix, respectively, in an adjusted volume of 12.5 μL for 90 min at 30°C, and reactions were stopped on ice. Luminescence measurements were performed using the *Gaussia*-Juice Luciferase Assay Kit (*pjk*) on a TECAN Infinite M1000 PRO. The luciferase activity was determined by adding 2 μL of the translation sample to a 96-well plate followed by injection of 50 μL freshly prepared reaction mix (1:50 coelenterazine: reaction buffer, *pjk*) and the integration time was 3 s. Each translation sample was assayed for luciferase activity in duplicate. Translational efficiency data were normalized to ARCA capped RLuc mRNA.

Immunoprecipitations and affinity pulldown

For immunoprecipitation of FLAG-tagged eIF4A versions, $4x10^6$ S2R+ cells each were transfected with ActC5-GAL4 and the corresponding pUAST attB-^{FLAG}eIF4A plasmids (or an empty vector) using Fugene reagent (Promega). After 48-72 hours, cells were washed with ice-cold PBS, lysed in 150 mM NaCl, 50 mM Tris/HCl pH 7.4, 2 mM $MgCl_2$, 1 mM EDTA, 1% Triton X-100, 0.5% deoxycholate, 5% glycerol and complete protease inhibitors for 20 minutes on ice. After clearing, lysates were incubated with anti-FLAG beads for 3 hours, washed three times with lysis buffer, and eluted with SDS loading buffer. Samples were analyzed by western blotting.

For eIF3b-RNA immunoprecipitations, $4x10^6$ S2R+ cells each were transfected with pUAST attB-5′UTR^{Mical}-GFP and empty pUAST attB (ratio 1:2 for low expression) using Fugene and grown for 48 to 72 hours. Cells were then mock-treated or treated with 0.3 μM RocA, washed with ice-cold PBS, and lysed in 200 mM NaCl, 25 mM Tris/HCl pH 7.4, 2 mM $MgCl_2$, 1 mM EDTA, 1% Triton X-100, 0.5 mM DTT and complete protease inhibitors for 20 minutes on ice. Lysates were then immunoprecipitated with 3 μL eIF3b serum (gift from M. Hentze, EMBL) or 3 μL control serum (unrelated preimmune) coupled to Dynabeads Protein G over night. Beads were washed three times with lysis buffer and once with PBS. 5%–10% of precipitates were removed and dissolved in SDS sample buffer for Western analysis, the rest of the beads was eluted with Trizol reagent to elute bound RNA according to the supplier's instructions. Bound RNA was reverse transcribed with a GFP-specific primer, and analyzed by GFP PCR.

In order to test for cap interaction of translation initiation factors, $8x10^6$ untransfected S2R+ cells were mock-treated or treated with 20 μM 20-hydroxyecdysone for 1 hour, washed with ice-cold PBS, and lysed in 200 mM NaCl, 50 mM Tris/HCl pH 7.4, 2 mM $MgCl_2$, 1 mM EDTA, 1% Triton X-100, 0.5% deoxycholate and complete protease inhibitors for 20 minutes on ice. After clearing by centrifugation, lysates were incubated with 20 μL m^7GTP agarose for 3 hours, and the beads were eluted with SDS sample buffer after three washes with lysis buffer.

Polysome profile

For polysome profiles from *Drosophila* S2R+ cells, $3x10^7$ cells each were grown for 48 hours. After mock treatment or treatment with with 0.3 μM RocA, the medium was removed, and cells were first washed with ice-cold PBS and frozen in liquid nitrogen. Frozen cells were then lysed on the plate in 10 mM Tris/HCl pH 7.5, 100 mM NaCl, 10 mM $MgCl_2$, 0.5 mM DTT, 1% Triton X-100, 0.5% deoxycholate, and 100 μg/ml cycloheximide and collected. After clearing by centrifugation, lysates were flash-frozen in liquid nitrogen. Samples were centrifuged on a 10 – 50% linear sucrose gradient in a TH-641/SW41 rotor (Thermo Scientific/Beckman Coulter), and gradients were fractionated using a density gradient fractionator (Isco) and a SYR-101 syringe pump (Brandel) with continuous monitoring of A254.

QUANTIFICATION AND STATISTICAL ANALYSIS

Imaging analysis

Pruning phenotypes in Figures 1, 2, 4, 6 and 7 were analyzed by counting the number of neurons that still had dendrites attached to the soma, these data were analyzed using a two-tailed Fisher's exact test. To assess severity, we also counted the number of primary and secondary branches still attached to the soma at 18 h APF. These data were analyzed using Wilcoxon's test.

GFP reporter fluorescence intensity in c4 da neurons (Figure 5; Figure S5) was measured on a Zeiss LSM710 confocal microscope under identical, nonsaturating conditions for each pair of manipulations and background was substracted. The relative reduction of reporter intensities by experimental manipulations compared to control were calculated as (1-(fluorescence^{exp}/fluorescence^{contr})*100. These data were compared by Wilcoxon's test. For tdtomato fluorescence, reporter fluorescence ratios of experimental and control RNAis was calculated and compared using a *Student's t test*.

Cell Reports, Volume *24*

Supplemental Information

Differential Requirement for Translation Initiation Factor Pathways during Ecdysone-Dependent Neuronal Remodeling in *Drosophila*

Sandra Rode, Henrike Ohm, Lea Anhäuser, Marina Wagner, Mechthild Rosing, Xiaobing Deng, Olga Sin, Sebastian A. Leidel, Erik Storkebaum, Andrea Rentmeister, Sijun Zhu, and Sebastian Rumpf

Rode Figure S1

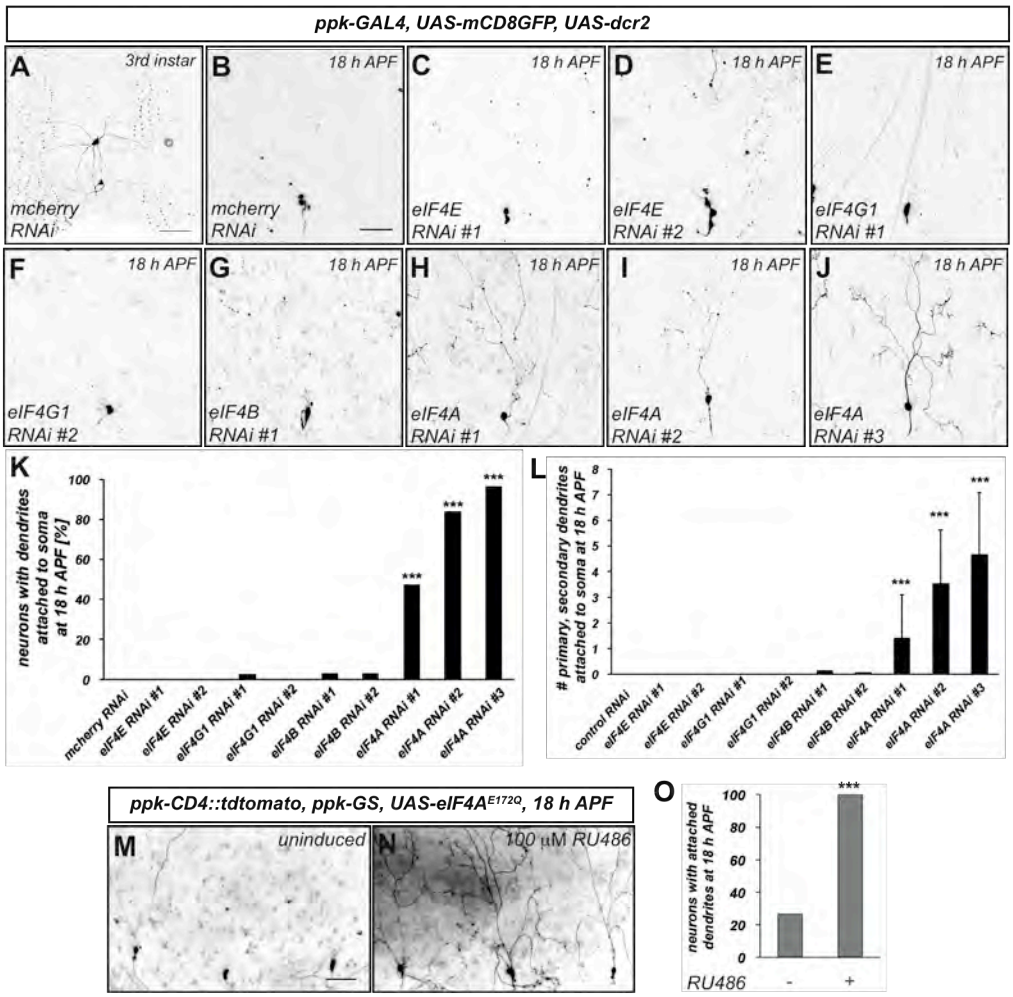

Figure S1 (related to Figure 1). eIF4A is the only eIF4F subunit required for c4da neuron dendrite pruning. A – J C4da neuron dendrite pruning. All neurons were labeled by CD8::GFP expression under *ppk-GAL4.* **A**, **B** Control c4da neurons (expressing mcherry RNAi) at the third larval instar stage (**A**). and at 18 hours after puparium formation (h APF) (**B**). **C** – **J** Effects of knockdown of eIF4F components on dendrite pruning at 18 h APF. **C**, **D** C4da neurons expressing eIF4E RNAis. **E**, **F** c4da neurons expressing eIF4G1 RNAis. **G** c4da neuron expressing eIF4B RNAi. **H** – **J** c4da neurons expressing eIF4A RNAis. **K** Penetrance of dendrite pruning defects in **B** – **J**. *** P<0.001, Fisher's exact test. **L** Number of attached primary and secondary dendrites at 18 h APF. Data are mean ± S. D., *** P<0.001, Wilcoxon's test. N=31-41. (See also Table S1). **M** – **O** eIF4A is acutely required for c4da neuron dendrite pruning. Larvae carrying drug-inducible *ppk-GeneSwitch* (*ppk-GS*) and UAS-eIF4A E172Q were kept on control food (**M**) or food containing 100 μM RU-486 (**B**) for 24 h prior to pupariation. C4da neurons were labeled with *ppk-CD4tdtomato* and dendrite pruning was assessed at 18 h APF. **O** Quantification of pruning defects in **M, N**. N=12-15, *** P<0.001, Fisher's exact test. Scale bars are 100 μm in **A** and 50 μm in **B** - **N**.

Supplemental_Table_S1 (related to Figure 1): Efficacy of used transgenic RNAi constructs

Genotype	Transforment ID	Lethality with act-GAL4
mCherry RNAi	BL 35785	no
eIF4E RNAi	BL 34096	yes
eIF4E RNAi	VDRC 7800	yes
eIF4G1 RNAi	VDRC 17003	yes
eIF4G1 RNAi	BL 33049	yes
eIF4B RNAi	BL 57305	no
eIF4B RNAi	VDRC 31364	no
eIF4A RNAi	VDRC 42202	yes
eIF4A RNAi	VDRC 42201	yes
eIF4A RNAi	BL 33970	yes

Rode Figure S2

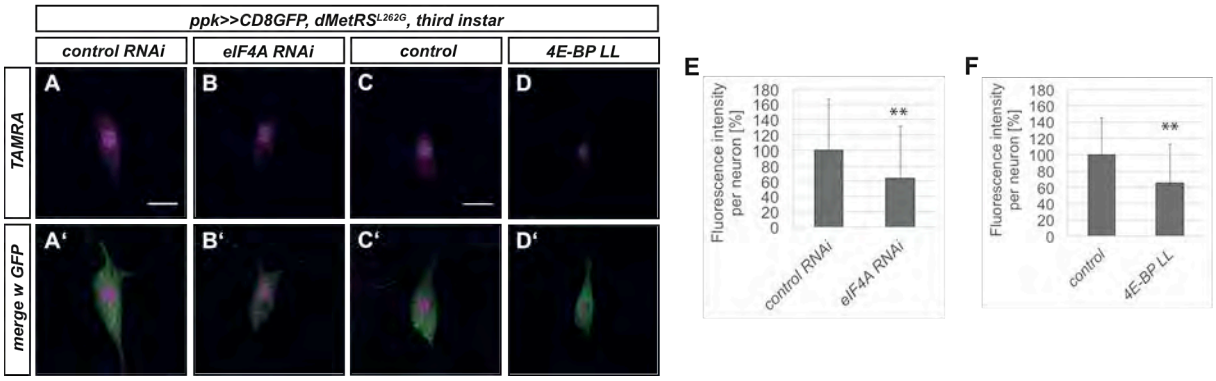

Figure S2 (related to Figure 2). eIF4A does not affect pruning via a global effect on translation. **A** – **D, A'** – **D'** FUNCAT labeling of newly synthesized proteins. dMARS^{ANL} expression in c4da neurons allowed incorporation of clickable azidonorleucine (ANL) into newly synthesized proteins which were then labeled covalently with TAMRA by FUNCAT. Upper panels (**A** – **D**) show TAMRA label of neurons of the indicated genotypes, lower panels (**A'** – **D'**) show the merge with CD8::GFP. **A**, **A'** C4da neuron expressing control mcherry RNAi. **B**, **B'** C4da neuron expressing eIF4A RNAi#1. **C**, **C'** C4da neuron expressing lacZ as a control. **D**, **D'** C4da neuron expressing constitutively active 4E-BP LL. **E** Quantification of signal intensity of experiments in **A** and **B**. **F** Quantification of signal intensity of experiments in **C** and **D**. ** P<0.01, Wilcoxon's test.

Rode Figure S3

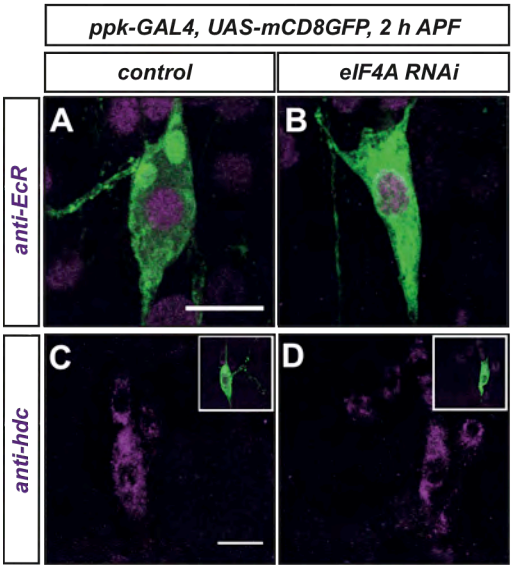

Figure S3 (related to Figure 3). EcR and hdc expression upon eIF4A RNAi. A, B Ecdysone receptor (EcR) expression in c4da neurons expressing a control RNAi (**A**) or eiF4A RNAi#1 (**B**) under *ppk-GAL4*. **C, D** Headcase (hdc) expression in c4da neurons expressing a control RNAi (**C**) or eiF4A RNAi#1 (**D**) under *ppk-GAL4*. Animals were stained with antibodies against the respective proteins at 2 h APF. Scale bars, 10 μm.

Rode Figure S4

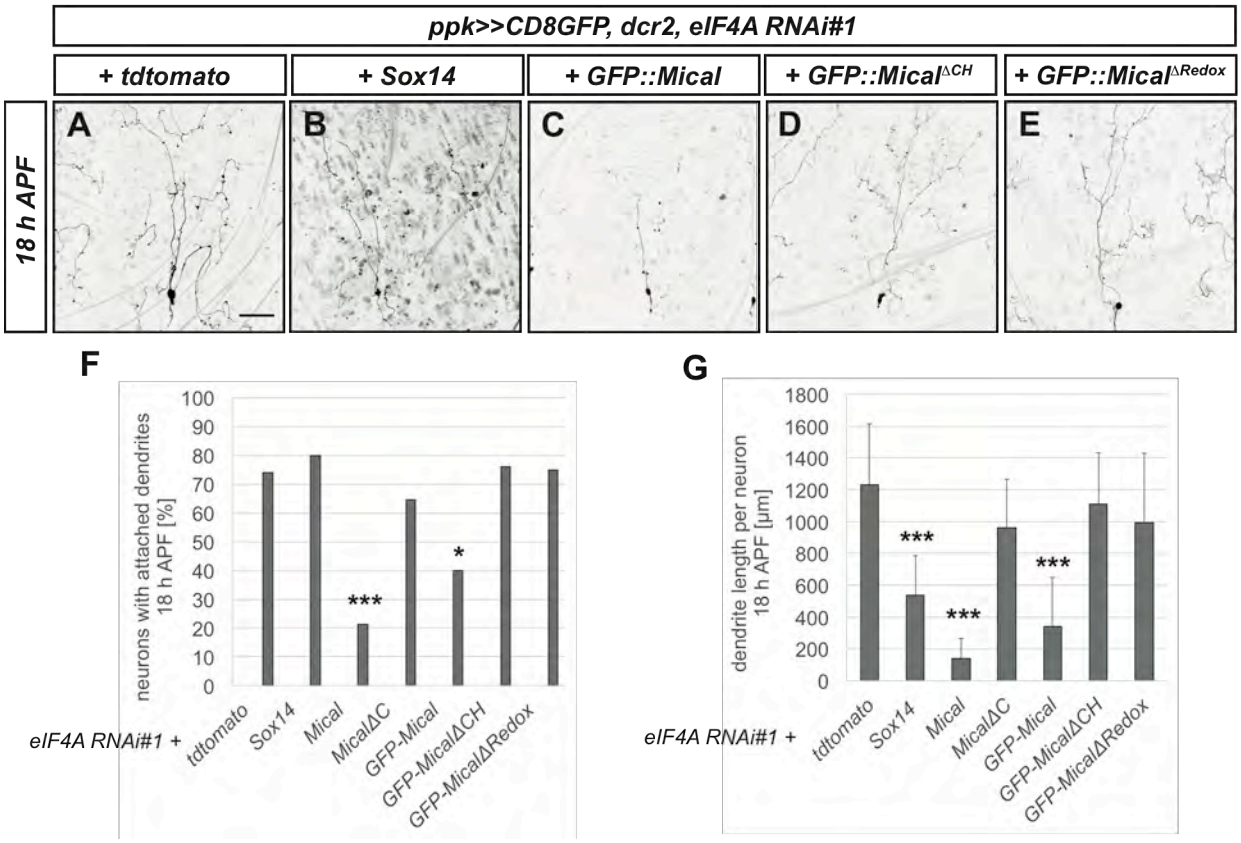

Figure S4 (related to Figure 4). Exogenous Mical, but not Sox14, rescues the pruning defects induced by eIF4A knockdown.

A – **E** The indicated UAS transgenes were coexpressed in c4da neurons with eIF4A RNAi#1 as in Figure 5. Shown are: C4da neurons coexpressing tdtomato as dosage control (same as in Figure 5) (**A),** Sox14 (**B**), full-length GFP::Mical (**C**), GFP::Mical lacking the *Calponin Homology* (CH) region (**D**), GFP::Mical lacking the flavooxygenase domain (ΔRedox) (**E**). **F** Penetrance of pruning defects (neurons with attached dendrites) in **A** – **E**. Included are also genotypes from Figure 5. *** P<0.001, * P<0.05 (using Fisher's exact test). N=12-32. **G** Length of unpruned dendrites at 18 h APF in **A** – **E**. *** P<0.001, * P<0.05 (Wilcoxon's test). Scale bars are 50 μm. Data represented in **I** are mean ± s.d..

Rode Figure S5

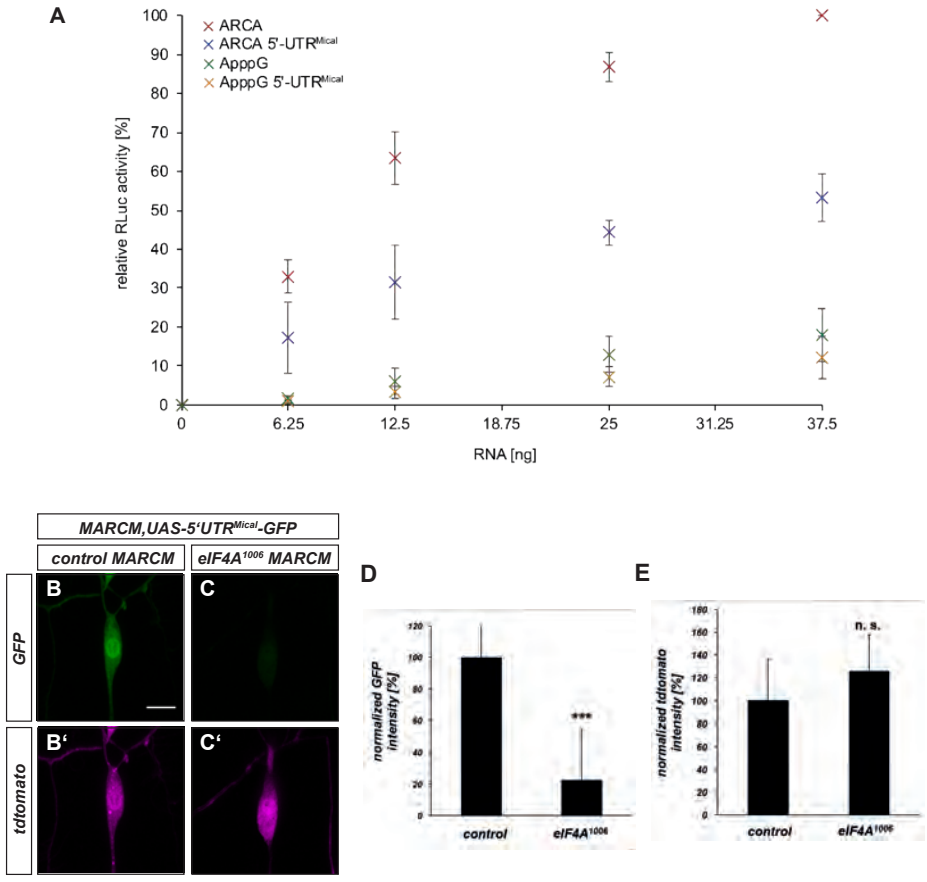

Figure S5 (related to Figure 5). Characterization of the Mical 5'UTR.

A Cap dependence of 5'UTR^{Mical}. Renilla Luciferase reporter mRNAs containing the active cap analogue ARCA or the control cap analogue ApppG were generated by in vitro transcription and assayed for translation efficiency by in vitro translation in reticulocyte lysate. Samples were: ARCA/ApppG, capped and uncapped reporters containing a control 5' UTR, ARCA 5'-UTR^{Mical}/ApppG 5'-UTR^{Mical}, capped and uncapped reporters containing the Mical 5' UTR. Different concentrations of mRNA were used, and luciferase activity was used for quantification. Data are averages of two independent experiments measured in duplicate. **B** – **C** Expression of *UAS-5'UTR^{Mical}-GFP* in third instar c4da neuron *eIF4A^{1006}* MARCM clones. Panels **B**, **C** show GFP signal, panels **B'**, **C'** show tdtomato signal in the same neuron. **B**, **B'** GFP and tdtomato in a control c4da MARCM clone. **C**, **C'** GFP and tdtomato in a *eIF4A^{1006}* c4da MARCM clone. **D** Quantification of GFP intensity. **E** Quantification of tdtomato intensity. ***P<0.001, Wilcoxon's test. Scale bars are 10 μm. Data represented are mean ± s.d..

Rode Figure S6

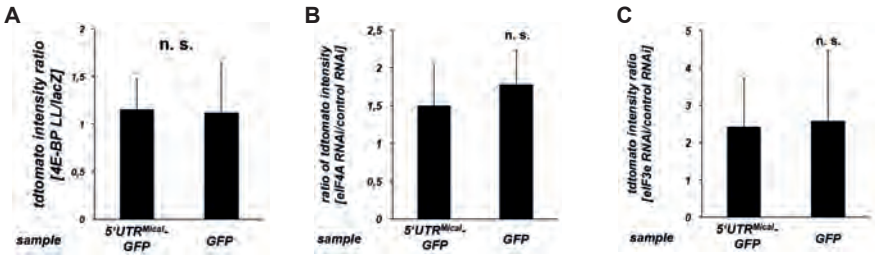

Figure S6 (related to Figure 5). Effects of initiation factor manipulations on tdtomato reporter fluorescence.

Tdtomato reporter fluorescence was measured as in Figure 5, and the ratios between experimental and control samples were taken. **A** 4E-BP^{LL} expression does not affect the tdtomato reporter activity (ratio ~1). **B**, **C** Knockdown of eIF4A (**B**) or eIF3e (**C**) increases fluorescence (ratios ~1.6 and ~2, respectively). These values are not significantly affected by the GFP reporter present.

Rode Figure S7

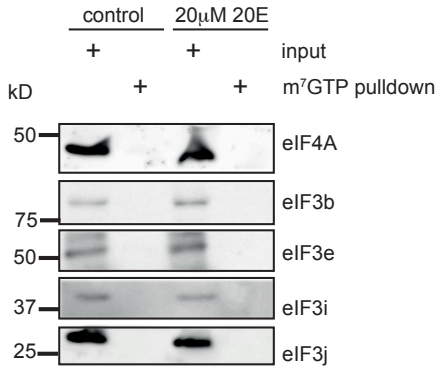

Figure S7 (related to Figure 6). Cap pulldown assay from S2 cell lysate.

Lysates from control S2 cells or S2 cells treated with 20 μM 20-hydroxyecdysone (20E) for one hour were incubated with m^7GTP agarose. After washes, bound proteins were eluted with SDS sample buffer and blotted against eIF4A or eIF3 subunits. Input and bound fractions are shown.